

Circuit Complexity in an interacting quenched Quantum Field Theory

Sayantana Choudhury^{1,*}, Rakshit Mandish Gharat^{2,†}, Saptarshi Mandal^{3,‡} and Nilesh Pandey^{4,§}

¹*Centre For Cosmology and Science Popularization (CCSP),*

SGT University, Gurugram, Delhi- NCR, Haryana- 122505, India,

²*Department of Physics, National Institute of Technology Karnataka, Surathkal, Karnataka-575025, India,*

³*Department of Physics, Indian Institute of Technology Kharagpur, Kharagpur-721302, India, and*

⁴*Department of Applied Physics, Delhi Technological University, Delhi-110042, India.*

In this work, we explore the effects of a quantum quench on the circuit complexity for a quenched quantum field theory having weakly coupled quartic interaction. We use the invariant operator method, under a perturbative framework, for computing the ground state of this system. We give the analytical expressions for specific reference and target states using the ground state of the system. Using a particular cost functional, we show the analytical computation of circuit complexity for the quenched and interacting field theory. Further, we give a numerical estimate of circuit complexity with respect to the quench rate, δt for two coupled oscillators. The parametric variation of the unambiguous contribution of the circuit complexity for an arbitrary number of oscillators has been studied with respect to the dimensionless parameter $(t/\delta t)$. We comment on the variation of circuit complexity for different values of coupling strength, different number of oscillators, and even in different dimensions.

I. Introduction

Recently, many of the works in theoretical physics are concerned with the confluence of various ideas in quantum many-body physics, quantum information theory and high energy physics [1–7]. Some of these works involved studying entanglement entropy in quantum systems, generally having a dynamical background [8–19]. Subsequently, it was discovered that entanglement entropy, although playing an important role in black-hole physics, is not sufficient to probe the interior of black holes. Susskind and collaborators, introduced a new measure in relation to the thermalisation properties of black holes, which was termed Quantum Computational Complexity (QCC) [20–27]. Lately, QCC has been studied widely in high energy physics. [28–83]. This stirred up exploring the QCC in the form of circuit complexity, in the context of free-field theories[84–86]. On the other hand, circuit complexity was computed for a weakly interacting field theory in [87].

Also, most of the recent works in many-body physics deal with dynamical systems where a time-dependent parameter is varied suddenly or very slowly. This is commonly referred to as a Quantum Quench. The quench protocol seemingly drives any out of equilibrium system and thermalises it[88–90]. Entanglement, in the context of quenched systems has been discussed in [18, 19, 91–98]. Recently, we have studied entanglement in a quenched two-body coupled oscillator system with a quartic coupling in [99]. Furthermore, circuit complexity for quenched systems was computed in [100, 101]. The ef-

fects of quenches in quantum systems have been explored experimentally for cold atoms in [102–111].

For dynamical systems, the time-dependent Schrodinger equation can be solved using Lewis-Resenfield invariant-operator method[112]. Lewis Resenfield method was used to determine the time-dependent eigenstates in [113–117]. Further, one can consider adiabatic evolution of time-dependent parameters[118, 119] and use invariant-operator method to compute time-independent perturbative corrections to the eigenstates [120]. The exact form of time-dependent parameters in such eigenstates can be evaluated by solving the Ermakov-Milne-Pinney [121–123] equation in Mathematica.

Motivated by all these ideas, in this work, we:

- start with discretising the Hamiltonian for an interacting Quantum Field Theory (QFT) with quartic coupling, on a finite-sized lattice, having a quenched frequency by using the most common protocol in the literature.
- use invariant operator method, in a perturbative framework, to fix the reference and target states which are chosen as the ground state for an interacting field theory (with quartic coupling).
- compute the circuit complexity for quenched-coupled oscillators by using Nielsen’s geometric approach [124–128] and choosing a specific cost function by modifying the results of [87].
- numerically evaluate the circuit complexity and comment on its parametric variation, for different cases

The organisation of the paper is as follows:

- Discretising, a Quantum Field Theory (QFT) with quartic interaction, on a lattice, we decouple the

* sayantan_ccsp@sgtuniversity.org,
sayanphysics@gmail.com

† rakshitmandishgharat.196ph018@nitk.edu.in

‡ saptarshihikra@gmail.com

§ nilesh911999@gmail.com

Hamiltonian using Fourier modes in section III. Evidently, the decoupled Hamiltonian refers to that of N coupled oscillators having a quartic perturbative coupling. The frequency of these oscillators is quenched by choosing a particular protocol.

- In section III, we use invariant operator method to compute the time-dependent ground states and also the first-order perturbative corrections to the ground state, for the quenched Hamiltonian.
- Using the ground, we fix a specific reference and target state in section IV. By using a particular cost function we compute the circuit complexity for the chosen reference and target states. The continuum limit of circuit complexity is also evaluated.
- In section V, we numerically evaluate circuit complexity for different sets of parameters and comment on the dynamical behavior of the circuit complexity in three different regimes.
- Section VI encapsulates the conclusions we draw from the results obtained in this work.

II. The Setup and the Quench protocol

As one of the first steps towards understanding circuit complexity in the context of quenched interacting field theory, in this section we begin with a scalar field theory with $\lambda\phi^4$ interaction term. We regulate this QFT by placing it on a lattice. Once discretized the Hamiltonian evidently represents a family of N coupled anharmonic oscillators. We transform the original coordinates to normal modes to decouple the Hamiltonian. This helps us to compute the eigenstates for the system in a much simpler way, which is discussed in the upcoming section. We follow the notations used in [87, 129] to facilitate an easy comparison. Further we mention the time-dependent quench profile chosen to be the frequency of these oscillators.

The Hamiltonian for a scalar field theory with a $\hat{\lambda}\phi^4$ interaction is given by [129],

$$\mathcal{H} = \frac{1}{2} \int d^{d-1}x \left[\pi(x)^2 + (\nabla\phi(x))^2 + m^2\phi(x)^2 + \frac{\hat{\lambda}}{12}\phi(x)^4 \right]. \quad (1)$$

Here d is the space-time dimensions. We assume that the coupling $\hat{\lambda} \ll 1$, so that we can work in a perturbative framework. This theory can be discretized on a $d - 1$ dimensional lattice, which is characterised by lattice spacing, δ . It can be shown that, the discretized

Hamiltonian becomes,

$$\mathcal{H} = \frac{1}{2} \sum_{\vec{n}} \left\{ \frac{\pi(\vec{n})^2}{\delta^{d-1}} + \delta^{d-1} \left[\frac{1}{\delta^2} \sum_i (\phi(\vec{n}) - \phi(\vec{n} - \hat{x}_i))^2 + m^2\phi(\vec{n})^2 + \frac{\hat{\lambda}}{12}\phi(\vec{n})^4 \right] \right\}. \quad (2)$$

Here \vec{n} denotes the spatial location of the points on lattice and \hat{x}_i represent the unit vectors along the lattice. Further, we introduce the following substitutions to simplify the form of the Hamiltonian:

$$\begin{aligned} \hat{X}(\vec{n}) &= \delta^{d/2}\phi(\vec{n}), & \hat{P}(\vec{n}) &= \pi(\vec{n})/\delta^{d/2}, \\ M &= \frac{1}{\delta}, & \omega &= m, \\ \eta &= \frac{1}{\delta}, & \lambda &= \frac{\hat{\lambda}}{24}\delta^{-d}, \end{aligned} \quad (3)$$

where ω represents the frequency of individual oscillators and η denotes inter-mass coupling. After these substitutions we get,

$$\begin{aligned} \mathcal{H} &= \sum_{\vec{n}} \left\{ \frac{\hat{P}(\vec{n})^2}{2M} + \frac{1}{2}M \left[\omega^2 \hat{X}(\vec{n})^2 \right. \right. \\ &\quad \left. \left. + \eta^2 \sum_i \left(\hat{X}(\vec{n}) - \hat{X}(\vec{n} - \hat{x}_i) \right)^2 \right. \right. \\ &\quad \left. \left. + 2\lambda \hat{X}(\vec{n})^4 \right] \right\}. \end{aligned} \quad (4)$$

The above Hamiltonian, in Eq.(4) represents a family of infinite coupled anharmonic oscillators. Setting $M = 1$, for simplicity the above Hamiltonian can be reformulated to that of N coupled oscillators with quartic perturbation:

$$H = \frac{1}{2} \sum_{a=0}^{N-1} [p_a^2 + \omega^2 x_a^2 + \eta^2 (x_a - x_{a+1})^2 + 2\lambda x_a^4]. \quad (5)$$

We use normal mode coordinates as discrete Fourier transform of the original coordinates, given by:

$$x_a = \frac{1}{\sqrt{N}} \sum_{k=0}^{N-1} \exp \left[i \frac{2\pi a}{N} k \right] \tilde{x}_k \quad (6)$$

$$p_a = \frac{1}{\sqrt{N}} \sum_{k=0}^{N-1} \exp \left[i \frac{2\pi a}{N} k \right] \tilde{p}_k \quad (7)$$

The Hamiltonian of Eq.(5) can be rewritten in normal modes as:

$$H = \frac{1}{2} \sum_{a=0}^{N-1} [p_a^2 + \omega^2 x_a^2 + \eta^2 (x_a - x_{a+1})^2 + 2\lambda x_a^4] \quad (8)$$

We split the above Hamiltonian into two parts,

$$H = H_k + H'_{\phi^4}, \quad (9)$$

where,

$$H_k = \frac{1}{2} \sum_{k=0}^{N-1} \left[|\tilde{p}_k|^2 + \omega_k^2 |\tilde{x}_k|^2 \right], \quad (10)$$

denotes the unperturbed (free) Hamiltonian which can be decoupled for each of the N oscillators. Here,

$$\omega_k^2 = \omega^2 + 4\eta^2 \sin^2 \left(\frac{\pi k}{N} \right), \quad (11)$$

denotes the frequency for each of the N oscillators. The exact form of the eigenstates for the unperturbed Hamiltonian of Eq.(10) has been computed in the subsection III A. On the other hand the $\lambda\phi^4$ perturbation term in the Hamiltonian of Eq.(9) can be dealt with by transforming the form of perturbations in normal modes:

$$H'_{\phi^4} = \frac{\lambda}{N} \sum_{k_1, k_2, k_3=0}^{N-1} \tilde{x}_\alpha \tilde{x}_{k_1} \tilde{x}_{k_2} \tilde{x}_{k_3}; \quad (12)$$

$$\alpha = N - k_1 - k_2 - k_3 \text{ mod } N$$

The contribution of the above Hamiltonian in Eq.(12) is evaluated by approximating the first order correction to the eigenstates of unperturbed Hamiltonian by employing the use of time-independent perturbation theory in the subsection III B.

We now consider the frequency ω in, Eq.(11) as a time-dependent quench profile. One of the most common quench profiles used in literature [130, 131] is given by:

$$\omega^2(t/\delta t) = \omega_0^2 \left[\tanh^2 \left(\frac{t}{\delta t} \right) \right]. \quad (13)$$

Here ω_0 can be considered as a free parameter and δt measures the quench rate. We choose this particular quench profile chosen since it admits an exact solution for the mode functions given in [130]. Note that this profile attains a constant value at very early and late time. Also, for this chosen form of quench profile, the dynamical changes in the system occur in the time window $[-\delta t, \delta t]$. We will set $t/\delta t = T$ and $\omega_0 = 1$. The respective frequencies in the normal mode basis take the following form,

$$\omega_k = \sqrt{\omega(T)^2 + 4\eta^2 \sin^2 \left(\frac{\pi k}{N} \right)}, \quad (14)$$

where $\omega(T)$ is the quench profile in Eq.(13) and k runs from 0 to $N - 1$.

As the frequency of each oscillator now depends on time, the unperturbed Hamiltonian is evidently time-dependent. We employ the use of invariant operator method to compute the exact form of the unperturbed Hamiltonian. We emphasise that the perturbed Hamiltonian is not time-dependent and hence can be used as a time-independent perturbation applied to N coupled oscillators. Using the ground state of total Hamiltonian of Eq.(8) we construct the reference as well as target states which are further used to evaluate the circuit complexity of this interacting quench model.

III. Constructing Wave function for a ϕ^4 quench model

In this section our prime objective is to derive an analytical expression for the eigenstates of Hamiltonian in Eq.(8), by using Lewis-Resenfield invariant operator method and approximate it to the first order perturbative correction. The expression for eigenstates of decoupled and unperturbed Hamiltonian in Eq.(10) is derived using invariant operator method, in the subsection III A. The first order perturbative correction to the ground state of the decoupled Hamiltonian, is derived in the subsection III B.

A. Eigenstates and Eigenvalues for unperturbed Hamiltonian

As shown earlier, in the normal mode basis, the unperturbed Hamiltonian, of Eq.(10), for N oscillators decouples. The wavefunction for N oscillators is then a product of eigenstates for each decoupled Hamiltonian, of Eq.(10).

$$\psi_{0,0,\dots,0}(\tilde{x}_0, \dots, \tilde{x}_{N-1}, T) = \psi_{n_1}(\tilde{x}_1, T) \psi_{n_2}(\tilde{x}_2, T). \quad (15)$$

Here T denotes the time-dependence of eigenstates emerging due to the quenched frequency from Eq.(13). We deal with these time-dependent eigenstates by employing the use of invariant operator method, closely following the prescription of [132]. Below, we have briefly mentioned the steps one can follow to compute analytical expression for eigenstates of a quenched Hamiltonian of Eq.(10). Note that we have suppressed the time-dependence of all the parameters to have simplicity in the notations.

First, we define the creation (a_k^\dagger) and annihilation (a_k) operators given by,

$$a_k = \frac{1}{\sqrt{2\dot{\gamma}_k}} \left[\dot{\gamma}_k \left(1 - i \frac{\dot{\rho}_k}{\rho_k \dot{\gamma}_k} \right) \tilde{x}_k + i \tilde{p}_k \right] \quad (16)$$

$$a_k^\dagger = \frac{1}{\sqrt{2\dot{\gamma}_k}} \left[\dot{\gamma}_k \left(1 + i \frac{\dot{\rho}_k}{\rho_k \dot{\gamma}_k} \right) \tilde{x}_k - i \tilde{p}_k \right].$$

Here, $k = 0, 1, \dots, N - 1$. Further, γ_k and ρ_k are time-dependent factors while $\dot{\gamma}_k = \partial_T \gamma_k$, $\dot{\rho}_k = \partial_T \rho_k$ and $\ddot{\rho}_k = \partial_T^2 \rho_k$. One can show that the operators in Eq.(16) satisfy the commutation relation $[a_i, a_j^\dagger] = \delta_j^i$. We fix the time-dependent factor ρ_k as the solution to the Ermakov-Milne-Pinney equation for each oscillator,

$$\ddot{\rho}_k + \omega_k^2 \rho_k = 0, \quad (17)$$

where ω_k denotes frequency for each coupled oscillator Eq.(14). If we define,

$$\alpha_k = \omega_0^2 + \frac{4\eta^2 \left(\sin^2 \left(\frac{\pi i}{N} \right) \right)}{\tanh^2(T)}, \quad (18)$$

for, $k = 0, 1, \dots, N - 1$, then using Eq.(13) one can rewrite Eq.(17) as:

$$\ddot{\rho}_k + \alpha_k \tanh^2(T)\rho_k = 0. \quad (19)$$

Here $k = 0, 1, \dots, N - 1$. We assume that the solution to Eq.(19) is of the form:

$$\rho_k(t, \delta t) = c_1 \epsilon_k^1(t, \delta t) + c_2 \epsilon_k^2(t, \delta t). \quad (20)$$

$$\epsilon_k^1 = \left(e^{\frac{2t}{\delta t}} \right)^{-\frac{1}{2} i \delta t \alpha_k} \left(e^{\frac{2t}{\delta t}} + 1 \right)^{\frac{1}{2} (\sqrt{1 - 4\delta t^2 \alpha_k^2} + 1)} {}_2F_1 \left(\frac{1}{2} \left(\sqrt{1 - 4\delta t^2 \alpha_k^2} + 1 \right), \frac{1}{2} \left(\sqrt{1 - 4\delta t^2 \alpha_k^2} - 2i\delta t \alpha_k^2 + 1 \right); 1 - i\delta t \alpha_k^2; -e^{\frac{2t}{\delta t}} \right), \quad (21)$$

where, ${}_2F_1$ denotes the hyper-geometric function. These complex valued solutions can be rewritten in the form $\epsilon_k^1 = \varepsilon_k + i\zeta_k$, where ε_k and ζ_k can be treated as real and linearly independent equations; for each $k = 0, \dots, N - 1$. As evaluated in [133], the solution to Eq.(19) is guaranteed to be of the form:

$$\rho_k(t, \delta t) = \sqrt{A\varepsilon_k^2(t, \delta t)t + 2B\varepsilon(t, \delta t)\zeta_k(t, \delta t) + C\zeta_k^2(t, \delta t)}. \quad (22)$$

Also, $\Omega_k = \rho_k^2 \dot{\gamma}_k$, is an invariant quantity with respect to time. Hence, γ_k can be computed as follows,

$$\gamma_k(t, \delta t) = \int_0^t \frac{\Omega_k}{\rho_k^2(t, \delta t)} dt. \quad (23)$$

Note that all the quantities are now a function of t and δt , this time-dependence is however suppressed along the most part of this article; until necessary. The creation and annihilation operators in Eq.(16) can now be used to construct invariant operator, for each of the N decoupled

$$u_{n_k} = \frac{1}{\sqrt{n!}} (a_k^\dagger)^n u_{0_k} = \left(\frac{1}{2^{n_k} n_k!} \right) \left(\frac{\gamma_k}{\pi} \right)^{1/4} \exp \left[\dot{\gamma}_k \left(1 - \frac{i\dot{\rho}_k}{\rho_k \dot{\gamma}_k} \right) \tilde{x} k^2 \right] \mathbf{H}_{n_k} \left[\sqrt{\gamma_k} \tilde{x}_k \right]. \quad (26)$$

Here \mathbf{H}_{n_k} denotes the Hermite polynomial of order n_k ; for each $k = 0, \dots, N - 1$. The eigenstates of the invariant operator shown in Eq.(26) are can now be used to compute the wavefunction for each decoupled Hamiltonian of Eq.(10) such that, $\psi_{n_k} = e^{i\beta_{n_k} u_{n_k}}$, where $\beta_{n_k} = -(1/2 + n_k)$; for $k = 0, \dots, N - 1$. The eigenstates for total unperturbed Hamiltonian of N coupled oscillators is then product for N copies of this wavefunc-

tion, Here c_1 and c_2 represent numerical constants. On the other hand ϵ_k^1 and ϵ_k^2 are two complex valued coefficients for each $k = 0, \dots, N - 1$. However we can consider only the term with, ϵ_k^1 as one of the solutions to Eq.(19), by setting $c_2 = 0$. Using Mathematica one can compute the exact form of ϵ_k^1 , following the steps shown in [99], which is mentioned below:

Hamiltonians, of Eq.(10):

$$I_k = \Omega_k \left(a_k^\dagger a_k + \frac{1}{2} \right). \quad (24)$$

Here, $k = 0, 1, \dots, N - 1$. Assuming that each invariant operator I_k is one of the complete set of commuting observables for the respective Hamiltonian H_k assures that each I_k has its own eigenstates. The ground state for this spectrum of each invariant operator can be computed using annihilation operator of Eq.(16) by solving, $a_k u_{0_k} = 0$. The expression for the ground state of for the spectrum of each invariant operator I_k of Eq.(24), for each $k = 0, 1, \dots, N - 1$ is given by,

$$u_{0_k} = \left(\frac{\dot{\gamma}_k}{\pi} \right)^{1/4} \exp \left[-\frac{\dot{\gamma}_k}{2} (1 - i\dot{\rho}_k \rho_k \dot{\gamma}_k) \tilde{x}_k^2 \right]. \quad (25)$$

The creation operator in Eq.(16) can then be used to evaluate the n_k^{th} eigenstate of the invariant-operator I_k which is given by,

tion,

$$\psi_{n_1 \dots n_{N-1}}^{(0)} = \prod_{k=0}^{N-1} \psi_{n_k}. \quad (27)$$

Using Eq.(26)) one can then show that,

$$\psi_{n_1 \dots n_{N-1}}^{(0)} = \left(\frac{1}{2^{n_0 + n_1 + \dots + n_{N-1}} n_0! \dots n_{N-1}!} \right) \left(\frac{g_0 g_1 \dots g_{N-1}}{\pi^N} \right)^{1/4} \exp \left[-\frac{i}{2} \sum_{k=0}^{N-1} (2n_k + 1) \gamma_k \right] \exp \left[-\frac{1}{2} \sum_{k=0}^{N-1} \tilde{\nu}_k \tilde{x}_k^2 \right] \times \mathbf{H}_{n_0} \left[\sqrt{\dot{\gamma}_0} \tilde{x}_0 \right] \dots \mathbf{H}_{n_{N-1}} \left[\sqrt{\dot{\gamma}_{N-1}} \tilde{x}_{N-1} \right]. \quad (28)$$

Here $g_k = \dot{\gamma}_k$ and,

$$\tilde{\nu}_k = \dot{\gamma}_k \left(1 - \frac{i\dot{\rho}_k}{\rho_k \dot{\gamma}_k} \right), \quad (29)$$

for $k = 0, 1, \dots, N-1$. We now focus on the ground state of the wavefunction shown in Eq.(28), which can be written as:

$$\psi_{0\dots 0}^{(0)} = \left(\frac{g_0 g_1 \dots g_{N-1}}{\pi^N} \right)^{1/4} \exp \left[-\frac{1}{2} \sum_{k=0}^{N-1} (i\gamma_k + \tilde{\nu}_k \tilde{x}_k^2) \right]. \quad (30)$$

Using the steps shown in [120] the energy eigenvalues for each of the N decoupled oscillators can be evaluated as,

$$\langle \psi_{n_k} | H_i | \psi_{n_k} \rangle = W_k(T) \left[n_k + \frac{1}{2} \right]. \quad (31)$$

Here $W_k(T)$ for $k = 0, \dots, N-1$ is a time-dependent factor for each oscillator given by,

$$W_k(T) = \frac{\dot{\gamma}_k}{2} \left(\frac{\dot{\rho}_k + \rho_i^2 \rho_i^2 + \rho_i^2 \dot{\gamma}_i}{\rho_i^2 \dot{\gamma}_i^2} \right). \quad (32)$$

Using the above form of time-dependent eigenvalues, one can compute the energy eigenvalues for the decoupled Hamiltonian of Eq.(10), which is given by:

$$\langle \psi_{n_1, \dots, n_{N-1}}^{(0)} | H | \psi_{n_1, \dots, n_{N-1}}^{(0)} \rangle = \sum_{k=0}^{N-1} W_k \left(n_k + \frac{1}{2} \right). \quad (33)$$

The above expression for the eigenvalues of unperturbed Hamiltonian can now be used to approximate the first order time-independent perturbative correction to the ground state of Eq.(30).

B. Wavefunction for $\lambda\phi^4$ perturbation applied to the ground state of N quenched-coupled oscillators

In this section our prime objective is to evaluate analytical expression for the wavefunction of ground state of N coupled oscillators in a perturbative framework, approximated to first order. We consider $\psi^{(1)}$ to be the first order correction arising due to Hamiltonian in Eq.(12). Hence, using Eq.(30), the expression for ground state of total Hamiltonian Eq.(8) corrected to first order in λ can be written as,

$$\psi_{0,0,\dots,0}(\tilde{x}_0, \dots, \tilde{x}_{N-1}) = \left(\frac{g_0 g_1 \dots g_{N-1}}{\pi^N} \right)^{1/4} \times \exp \left[-\frac{1}{2} \sum_{k=0}^{N-1} (i\gamma_k + \tilde{\nu}_k \tilde{x}_k^2 + \lambda \psi^{(1)}) \right]. \quad (34)$$

We take note of the fact that for N coupled oscillators the $\lambda\phi^4$ perturbation can give rise to a combination of five terms viz., $x_a^4, x_b^2 x_c^2, x_d x_e^3, x_f x_g^2 x_h$ and $x_i x_j x_k x_l$. Hence, we have expressed the form of first order correction by closely following the notations used in [87],

$$\begin{aligned} \psi_4^1 = & \sum_{\substack{a=0 \\ 4a \bmod N \equiv 0}}^{N-1} B_1(a) + \sum_{\substack{b,c=0 \\ (2b+2c) \bmod N \equiv 0 \\ b \neq c}}^{N-1} \frac{B_2(b,c)}{2} + \sum_{\substack{d,e=0 \\ (3e+d) \bmod N \equiv 0 \\ d \neq e}}^{N-1} B_3(d,e) \\ & + \sum_{\substack{f,m,h=0 \\ (f+2m+h) \bmod N \equiv 0 \\ f \neq m \neq h}}^{N-1} \frac{B_4(f,m,h)}{2} + \sum_{\substack{i,j,k,l=0 \\ (i+j+k+l) \bmod N \equiv 0 \\ i \neq j \neq k \neq l}}^{N-1} \frac{B_5(i,j,k,l)}{24}. \end{aligned} \quad (35)$$

One can compute the exact form of coefficients for each of the five different perturbative terms by first choosing appropriate number of oscillators and then generalising the result for N oscillators. Further one can compute the

perturbative correction by setting V as each perturbative term mentioned above, and then using the formula given below,

$$\psi_{0,\dots,0}^{(1)} = \sum_{(n_0 \dots n_{N-1}) \neq (0, \dots, 0)} \frac{\langle \psi_{n_0, \dots, n_{N-1}}^{(0)} | V | \psi_{0, \dots, 0}^{(0)} \rangle \times \psi_{n_0, \dots, n_{N-1}}^{(0)}}{\langle \psi_{0, \dots, 0}^{(0)} | H | \psi_{0, \dots, 0}^{(0)} \rangle - \langle \psi_{n_0, \dots, n_{N-1}}^{(0)} | H | \psi_{n_0, \dots, n_{N-1}}^{(0)} \rangle}. \quad (36)$$

For example, if one wants to get the form of $B_3(d,e)$

in Eq.(35), set number of oscillators to $N = 2$ and put

$V = x_0 x_1^3$ in Eq.(36). The form of the perturbative expansion thus obtained can be generalised for arbitrary number of, N oscillators. We then repeat these steps to fix all the coefficients of perturbative expansion. The exact form of all these coefficients, using Eq.(36) is tabulated in Appendix C.

IV. Analytical calculation for Circuit Complexity of ϕ^4 quench model

The ground state of the total Hamiltonian, calculated in the previous section, given by Eq.(34) is used to construct the reference and target states in the subsection IV A. Choosing a specific cost functional, we have derived the analytical expression for circuit complexity, by modifying the results of [87], in the subsection IV B.

A. Constructing Target/Reference states

In the wavefunction for N oscillators with quartic perturbation shown in Eq.(34) following the prescription given in [87] one can write the exponent in the form of a matrix conjugated by a basis vector, \vec{v} . The wavefunction then takes the below given form:

$$\psi_{0,0,\dots,0}^s(\tilde{x}_0, \dots, \tilde{x}_{N-1}) \approx \mathcal{N}^s \exp \left[-\frac{1}{2} v_a A_{ab}^s v_b \right]. \quad (37)$$

Here \mathcal{N}^s denotes the normalisation factor and A^s denotes a block diagonal matrix, for the respective state. Further, the space of circuits is parameterised by setting value of the running parameter s . At $s = 1$ the above form of wavefunction coincides with the wavefunction in Eq.(34) such that $\mathcal{N}_{s=1}$ becomes the normalising factor of Eq.(34), by an appropriate choice of the basis \vec{v} . Then $\psi_{0,0,\dots,0}^{s=1}$ is referred to as the target state. There are many possible choices for choosing bases so as to obtain the terms in perturbative expansion in Eq.(35). However as a minimal choice we choose the below mentioned basis,

$$\vec{v} = \{\tilde{x}_0, \dots, \tilde{x}_{N-1}, \tilde{x}_0^2, \dots, \tilde{x}_{N-1}^2, \dots, \tilde{x}_a \tilde{x}_b, \dots\}. \quad (38)$$

In this basis one can show that the matrix A , in Eq.(37) has a block diagonal form:

$$A_{ab}^{s=1} = \begin{pmatrix} A_1 & 0 \\ 0 & A_2 \end{pmatrix}. \quad (39)$$

A_1 contains coefficients of terms like x_a^2 and $x_a x_b$ in Eq.(34) multiplied by -2 . All the elements of A_1 can be fixed to obtain a specific form of target state. This block is often referred to as the *unambiguous* block.

The elements of A_2 block consist of coefficients which are basis dependent i.e. there is not any unique choice

of basis vector for defining the elements of A_2 block because unlike A_1 block which only consist of coefficients of quadratic terms and they can be defined uniquely without any ambiguity, the A_2 block consists of elements which are coefficients of terms like $\tilde{x}_a^2 \tilde{x}_b^2$, $\tilde{x}_a^2 \tilde{x}_b^2 \tilde{x}_c^2$, $\tilde{x}_a \tilde{x}_b \tilde{x}_c \tilde{x}_d$ which can be defined in several ways. Due to this arbitrariness, the complexity for the ambiguous block will be different for different choices of basis. One cannot therefore fix elements of A_2 such that the contribution of A_2 to total complexity of the system is independent of choice of basis. Due to these ambiguities, the A_2 block is often referred to as *ambiguous* block. We construct the reference state by choosing the value of all the frequencies for each of the N oscillators as $\tilde{\omega}_{ref}$. Since all the oscillators have same frequency, the reference state evidently would be time-independent. Then wavefunction in Eq.(35) can be modified to that of reference state, mentioned below,

$$\psi^{s=0}(x_1, x_2, \dots, x_n) = \mathcal{N}^{s=0} \exp \left[-\sum_{i=0}^{N-1} \frac{\tilde{\omega}_{ref}}{2} (x_i^2 + \lambda^0 x_i^4) \right]. \quad (40)$$

Note that, λ^0 is a parameter denoting the non-Gaussian nature of the reference state and is not to be confused with the perturbative coupling λ used in target state. In normal modes the above expression can be recast as shown below,

$$\psi^{s=0}(\tilde{x}_1, \tilde{x}_2, \dots, \tilde{x}_n) = \mathcal{N}^{s=0} \exp \left[-\frac{1}{2} (v_a A_{ab}^{s=0} v_b) \right], \quad (41)$$

where the matrix $A_{ab}^{s=0}$ can be fixed as:

$$A_{ab}^{s=0} = \begin{pmatrix} \tilde{\omega}_{ref} \mathbb{1}_{N \times N} & 0 \\ 0 & A_2^{s=0} \end{pmatrix}. \quad (42)$$

Again there will be ambiguities in fixing the elements of $A_2^{s=0}$ for the reasons already mentioned above. Equipped with the target and reference states for the quenched and interacting oscillators we can proceed to give an analytical expression for circuit complexity by getting around the ambiguities in the upcoming subsection.

B. Analytical calculation of the complexity functional

In this subsection we outline analytical steps to compute the expression for circuit complexity for the previously mentioned target state Eq.(34) starting with a reference state Eq.(41) using the results of [87]. As shown in [100] the complexity functional depends on the chosen cost function. In this article we work with the following cost function,

$$\mathcal{F}_\kappa(s) = \sum_I p_I |Y^I|^\kappa. \quad (43)$$

As shown in [80, 87] the circuit complexity with this particular cost function becomes,

$$\mathcal{C}_\kappa = \int_{s=0}^1 \mathcal{F}_\kappa ds. \quad (44)$$

Next, we write the complexity as sum of two terms,

$$\mathcal{C}_\kappa = \mathcal{C}_\kappa^{(1)} + \mathcal{C}_\kappa^{(2)}. \quad (45)$$

Here $\mathcal{C}_\kappa^{(1)}$ refers to the contribution to the circuit complexity from A_1 block while $\mathcal{C}_\kappa^{(2)}$ refers to the contribution from A_2 block. $\mathcal{C}_\kappa^{(1)}$ and $\mathcal{C}_\kappa^{(2)}$ can be given as ratio of eigenvalues of the respective blocks for chosen target (34) and reference states Eq.(41) as prescribed in [87, 100],

$$\mathcal{C}_\kappa = \frac{1}{2^\kappa} \sum_{i=0}^{N-1} \left| \log \left(\frac{\Lambda_i^{(1)}}{\tilde{\omega}_{ref}} \right) \right|^\kappa + \mathcal{A} \sum_j \left| \log \left(\frac{\Lambda_j^{(2)}}{h_i \tilde{\omega}_{ref} \lambda_0} \right) \right|^\kappa. \quad (46)$$

Here \mathcal{A} denotes the penalty factor. Due to the ambiguities arising while fixing the form of A_2 block, numerically one cannot fix the form of $\Lambda_i^{(2)}$. However, as discussed in the Appendix B we can choose a minimal basis such that elements of A_2 are fixed for $N = 2$ oscillators. In the Appendix B, we have computed the total circuit complexity for $N = 2$ coupled oscillators having a quenched Hamiltonian with a quartic coupling.

In this work, have neglected the contribution of the ambiguous block i.e. $\mathcal{C}_\kappa^{(2)}$ as we cannot find any basis to get the numerically exact contribution of A_2 block for arbitrary number of oscillators. Nonetheless, we attempt to give an analytical form of $\mathcal{C}_{\kappa=1}^{(2)}$ in terms

$$\Lambda_i = \frac{3\lambda\rho_i^2}{2N} \left(\frac{g_\alpha + 2g_i}{g_\alpha(\rho_i^2(g_i + \omega_i^2) + \dot{\rho}_i)} - \frac{2g_i\rho_\alpha^2}{\rho_i^2(\rho_\alpha^2(\omega_i^2 g_\alpha + g_i(2g_\alpha + \omega_\alpha^2)) + g_i\rho_\alpha) + \dot{\rho}_i g_\alpha \rho_\alpha^2} \right) + \frac{\tilde{\nu}_i}{2}, \quad N: \text{ Even} \quad (48)$$

$$= \frac{3\lambda g_i^2 \rho_i^4 ((g_i + \omega_i^2) \rho_i^2 + \dot{\rho}_i)}{N g_i (\rho_i^2 (g_i + \omega_i^2) + \dot{\rho}_i) (\rho_i^2 (\rho_i^2 (g_i \omega_i^2 + g_i (2g_i + \omega_i^2)) + g_i \dot{\rho}_i) + g_i \dot{\rho}_i \rho_i^2)} + \frac{\tilde{\nu}_i}{2}, \quad N: \text{ Odd}$$

where the index, $\alpha = |N/2 - i|$. One can insert this expression for eigenvalues in Eq.(46) to get the desired value of circuit complexity. We emphasize that the form of these eigenvalues make the circuit complexity a time-dependent quantity due to the chosen quench profile. This time-dependence of complexity is explored in numerical plots by choosing an appropriate scale of time. One can check the behaviour of circuit complexity, \mathcal{C}_1 at the continuum limit: $N \rightarrow \infty$ while $\delta \rightarrow 0$ such that $L = (N\delta)$ is finite.

Now, in arbitrary dimensions, the equation for $\mathcal{C}_{\kappa=1}^{(1)}$, can

of renormalized parameters in the Appendix A again following the steps shown in [87].

C. The Continuum Limit for \mathcal{C}_1

Now, we will compute the exact form of eigenvalues of A_1 block, taking the continuum limit. To find the form of $\Lambda_i^{(1)}$, we now reinstate the factor of M previously set to $M = 1$ in the section II. In light of this the Hamiltonian, given in Eq.(8) will change, although retaining the previous form of eigenvalues and eigenfunctions. The new Hamiltonian with a factor of M becomes,

$$H = \frac{1}{M} \sum_{\vec{n}} \left\{ \frac{P(\vec{n})^2}{2} + \frac{1}{2} M^2 \left[\omega^2 X(\vec{n})^2 + \Omega^2 \sum_i (X(\vec{n}) - X(\vec{n} - \hat{x}_i))^2 + 2\{\lambda_4 X(\vec{n})^4\} \right] \right\}. \quad (47)$$

Considering the reinstated factor of M , we rescale some of the parameters as shown below,

$$\omega \rightarrow \frac{\omega}{\delta}; \quad \eta \rightarrow \frac{\eta}{\delta}; \quad \lambda \rightarrow \frac{\lambda}{\delta^2}; \quad \tilde{\omega}_{ref} \rightarrow \frac{\tilde{\omega}_{ref}}{\delta}; \quad \lambda^0 \rightarrow \frac{\lambda^0}{\delta}.$$

Using these rescaled parameters one can generalise the form of eigenvalues $\Lambda_i^{(1)}$ using Mathematica by considering trial cases for different values of N and eliminating all the factors aside for ρ_k and $\tilde{\omega}_k$ by using appropriate formulae mentioned in previous sections. Below we show the generalised formula for eigenvalues of $A_1^{(s=1)}$ block depending on whether the chosen number of oscillators, N is even or odd,

be rewritten as:

$$\mathcal{C}_{\kappa=1}^{(1)} = \frac{1}{2} \sum_{k=1}^{d-1} \sum_{i=0}^{N-1} \left| \log \left(\frac{\Lambda_i^{(1)}}{\tilde{\omega}_{ref}} \right) \right|. \quad (49)$$

For simplicity, if one chooses to set same frequency (of the respective oscillator) in each dimension, d , then one can write:

$$\omega_i = \sqrt{\frac{1}{d-1} \left[4(d-1)\eta^2 \sin^2 \left(\frac{\pi i}{N} \right) + \omega_0^2 \tanh^2 \left(\frac{t}{\delta t} \right) \right]}. \quad (50)$$

Hence, in arbitrary dimensions d , the circuit complexity can be still be computed using Eq.(46), thus getting rid

of the lattice sums in Eq.(49) such that frequencies are set to Eq.(50).

V. Numerical Results

In this section we numerically evaluate the value of circuit complexity for coupled oscillators using the expressions computed for total complexity of two coupled oscillators, denoted by \mathcal{C} , shown in the Appendix B and the unambiguous contribution of complexity for arbitrary number of oscillators using the results of the subsection IV C, henceforth denoted by C_1 . Note that each time-dependent coefficients in these expressions explicitly depend on $\rho_k(t, \delta t)$ given by Eq.(22). To obtain the values of A, B and C which can be inserted in Eq.(22), we set some straightforward initial conditions. The invariant quantities, Ω_k in Eq.(23) are taken to be $\Omega_k = 1$. Using the values of $\rho_k(t, \delta t)$ for $t \rightarrow 0$, we get the desired values of A, B and C by setting $\rho_k(0, \delta t) = 1$ while $\gamma_k(0, \delta t) = 0$ by using $AC - B^2 = \Omega^2$. The coupling between the oscillators is set to be $\eta = 0.25$. The free parameter in the quench profile, Eq.(13) is set to $\omega_0 = 1$. The frequency of reference state is set to $\omega_{ref} = 0.001$.

Using the exact values of circuit complexity we parameterise four different plots in this section. The first plot features the behaviour of total complexity \mathcal{C} computed for two coupled oscillators discretised on a lattice of size $L = 20$, varying with the quench rate δt . This plot is divided into two regions, $\delta t < 1$ is the sudden quench limit (blue) region while $\delta t > 1$ is the slow quench limit (yellow) region. The next three plots characterise the behaviour of unambiguous contribution of circuit complexity C_1 for more than two coupled oscillators discretised on a lattice of size, $L = 100$, varying with dimensionless parameter $(t/\delta t)$. In these plots we mark $(t/\delta t) = 1$ as Quench Point, by a dotted vertical red line. The red region for $(t/\delta t) < 1.2$ features the early time behavior of circuit complexity, the yellow region $0.8 < (t/\delta t) < 1.2$ shows the behavior of complexity near the quench point while the blue region, $(t/\delta t) > 1.2$ characterises the late time behavior of circuit complexity.

In Fig.1, we have plotted the numerical values of total complexity for $N = 2$, coupled oscillator system with quartic interaction, using Eq.(B7), with respect to the quench rate δt . The blue coloured region shows the behaviour of circuit complexity in the fast regime, $\delta \ll 1$. In slow regime, initially, the circuit complexity monotonically increases till $\delta t = 0.01$. Beyond, $\delta t = 0.01$ the complexity shows a linear scaling with slope, $\log \mathcal{C} / \log \delta t = 0.0825$, upto $t = 0.1$. This linear scaling is then followed by a monotonous increase in circuit complexity till $t = 0.2$. Beyond $t = 0.2$, circuit complexity saturates, making transition into slow regime, $\delta t > 1$, marked by a yellow background. Furthermore, it is evident that, for each quartic coupling, λ , the circuit complexity shows same behaviour. However, it is clear

that as λ increases quartic coupling, the complexity decreases.

Although one cannot get numerical results for total circuit complexity of more than two oscillators, we have plotted the numerical values of complexity pertaining to the unambiguous block i.e., C_1 with respect to the dimensionless parameter $(t/\delta t)$ for $N = 10$ coupled oscillators, in Fig.2. The figure is divided into three regions, first is the early time behaviour for the dimensionless parameter between $0 < (t/\delta t) < 0.8$ marked by a red background. In this region for all the three considered quartic couplings, circuit complexity decreases linearly upto $(t/\delta t) = 0.7$. Beyond this, for $(t/\delta t) > 0.7$, circuit complexity C_1 , diverges for each particular quartic coupling λ , such that higher the value of λ , higher is the complexity C_1 . This linear scaling is then followed by a monotonous decrease in the value of C_1 , as we move near the quench point $(t/\delta t) = 1$, marked by a yellow background. The late time behaviour, is characterised by saturation of C_1 , for $(t/\delta t) > 1.2$, which is marked by a blue background. It is evident that for different quartic couplings, λ , the circuit complexity C_1 scales similarly in each particular region. However as we increase the quartic coupling, λ , circuit complexity C_1 increases at any particular time near and beyond the quench point.

In Fig.3 we have plotted the unambiguous contribution of circuit complexity C_1 for a discretised field theory with respect to the dimensionless parameter $(t/\delta t)$ for different number of oscillators, viz., $N = 10, 11, 12$ (keeping quartic coupling fixed at $\lambda = 0.01$). The early time behavior for a particular N is characterised by a steep linear decrease in value of circuit complexity, C_1 upto $(t/\delta t) = 0.4$. Beyond this point the complexity C_1 monotonically decreases and finally saturates at $(t/\delta t) \approx 0.5$. After this point, the unambiguous contribution of circuit complexity, C_1 remains saturated. The early time behavior of C_1 featuring a decrease and saturation in value of complexity is marked by red background. The behavior of C_1 near to the quench point as well as at late time is characterised by a constant saturated value at all times, marked by yellow and blue backgrounds respectively. It is evident that unambiguous contribution of circuit complexity, C_1 scales similarly for any N . However larger the number of oscillators N , larger is the value of C_1 . In the continuum limit when we have large number of coupled oscillators, one can expect that the unambiguous contribution of circuit complexity, C_1 will behave similar to that shown in this figure.

In Fig.4, we have plotted the unambiguous contribution of circuit complexity C_1 for a discretised field theory with respect to the dimensionless parameter $(t/\delta t)$ for different number of dimensions, viz., $d = 2, 3, 4$ (keeping quartic coupling fixed at $\lambda = 0.01$ while number of oscillators $N = 10$). For a particular d , the early time behavior of unambiguous contribution of circuit complexity is characterised by a monotonous decrease in the value of C_1 , marked by a red background. The values of C_1 for different dimensions, d begin to converge near to the

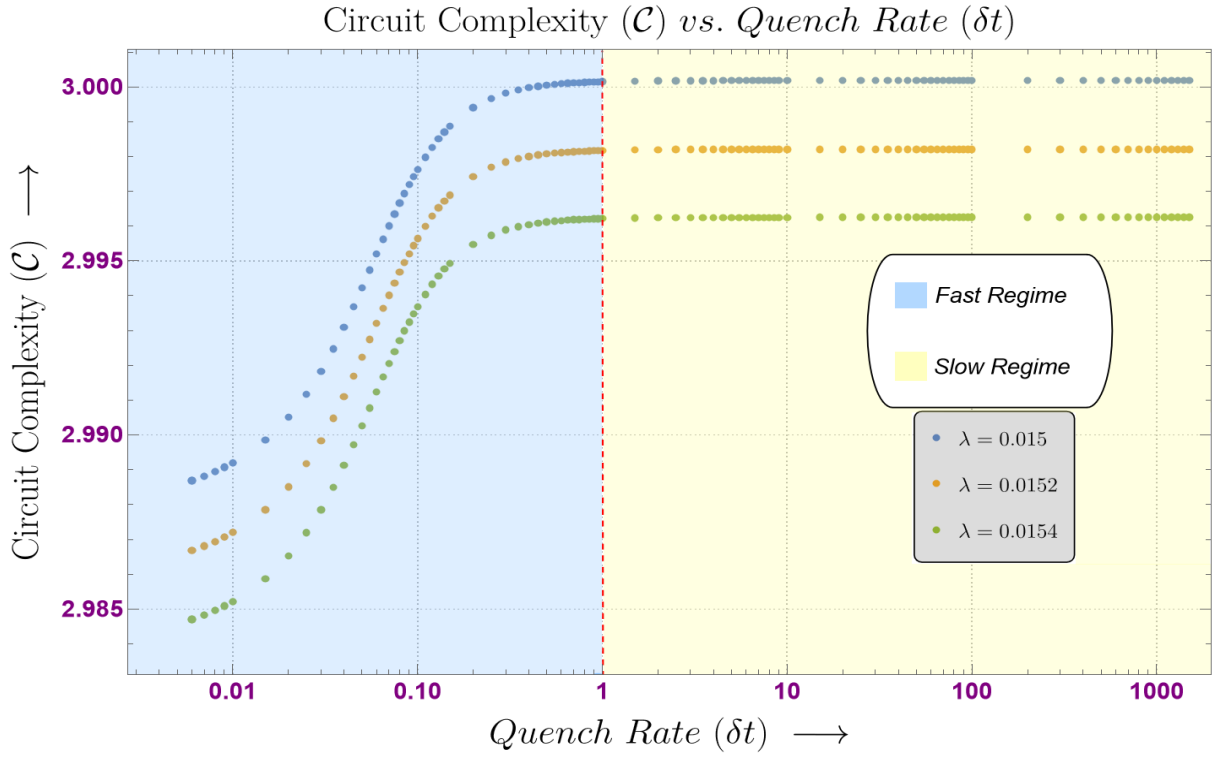


FIG. 1. Log-Log variation of the total circuit complexity (\mathcal{C}) with respect to the quench rate (δt) for different orders of the coupling constant λ for two coupled oscillators with quartic perturbation.

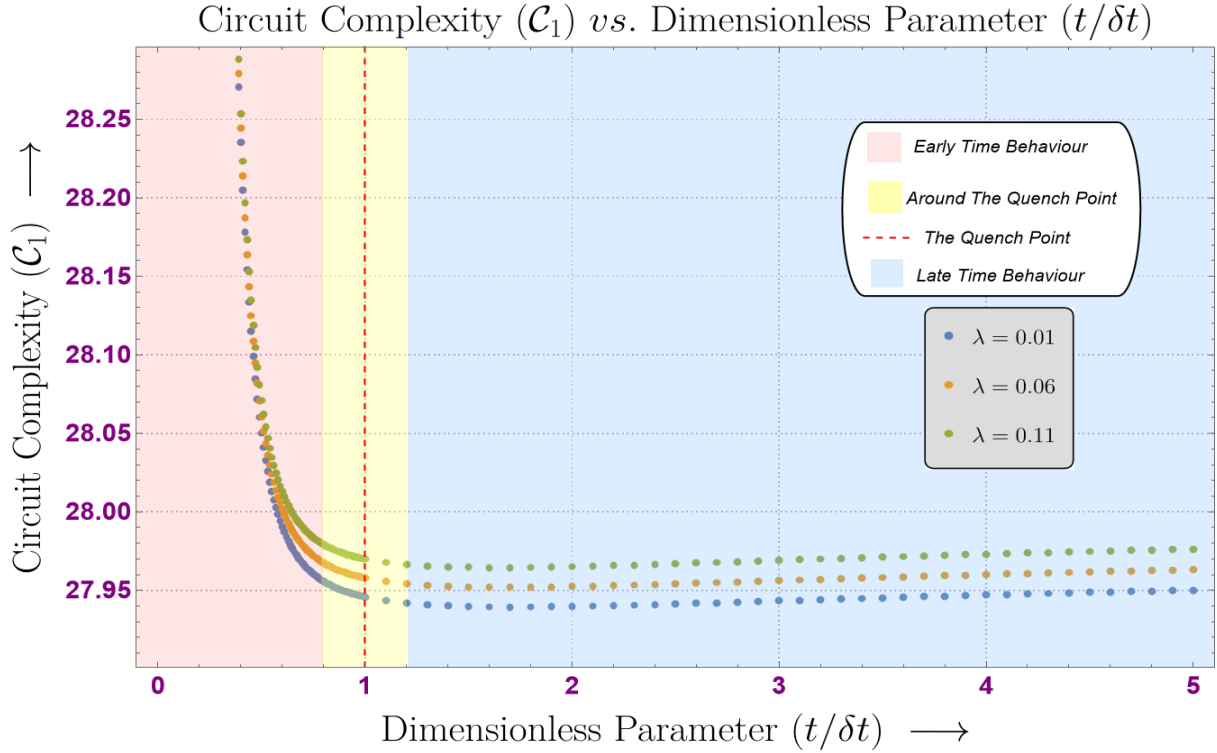


FIG. 2. Variation of the circuit complexity for A_1 block (\mathcal{C}_1) for $N = 10$, with respect to the dimensionless parameter ($t/\delta t$) for different orders of the coupling constant λ .

quench point ($t/\delta t = 1$) and finally saturate to a constant value, this is marked by yellow background. At

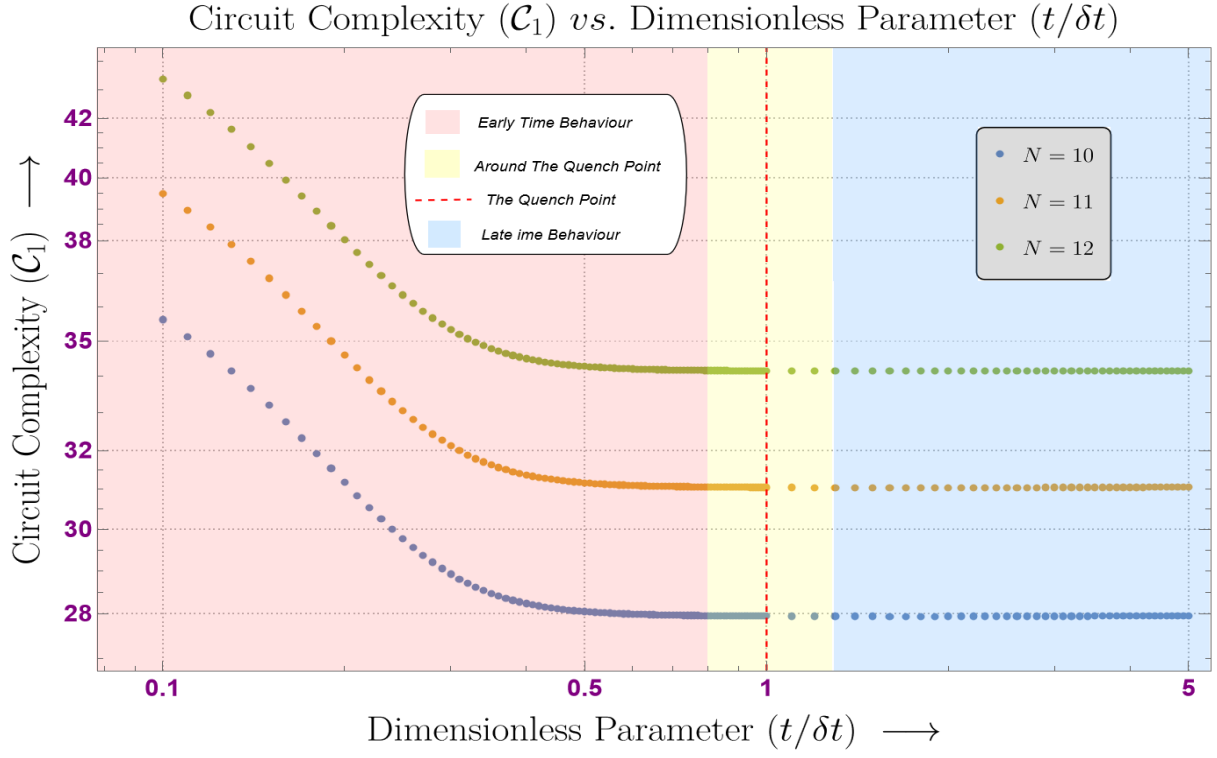


FIG. 3. Semi-Log variation of the circuit complexity for A_1 block (\mathcal{C}_1) at $\lambda = 0.01$, with respect to the dimensionless parameter ($t/\delta t$) for different values of N .

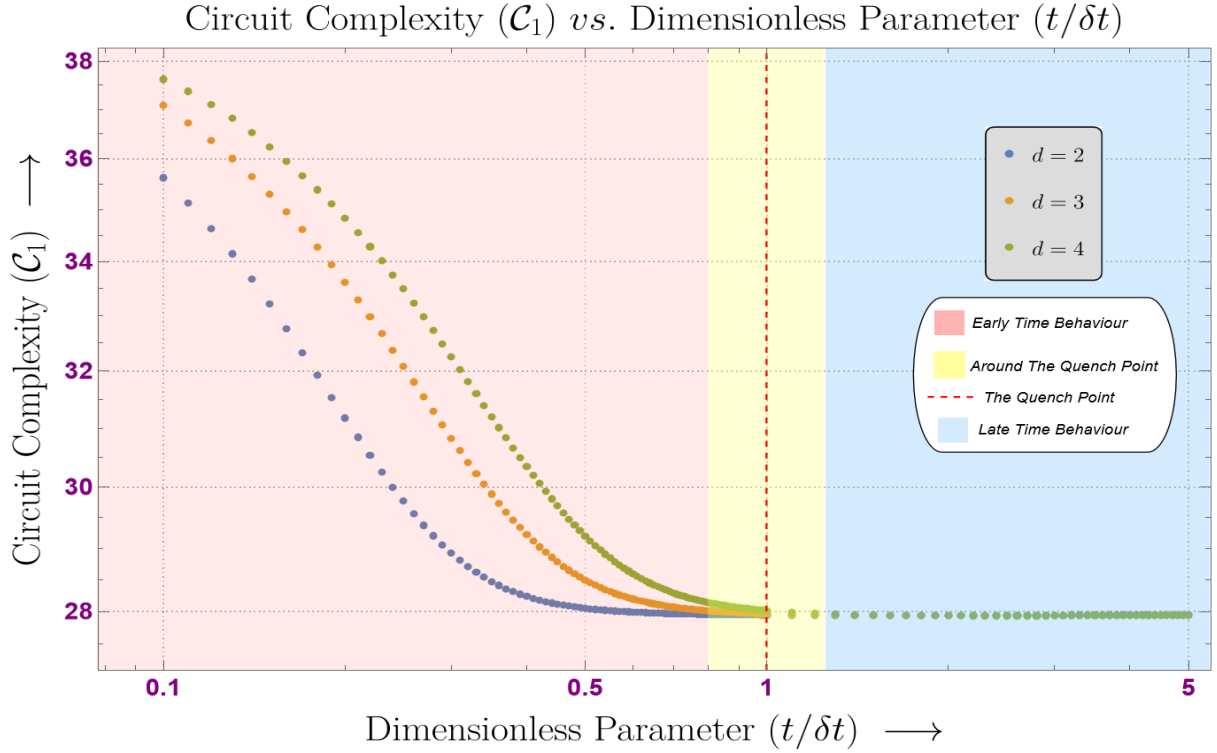


FIG. 4. Semi-Log variation of the circuit complexity for A_1 block (\mathcal{C}_1) at $\lambda = 0.01$, $N = 10$ with respect to the dimensionless parameter ($t/\delta t$) for different dimensions d .

late times, the unambiguous contribution of circuit complexity \mathcal{C}_1 remains saturated to a constant value, this

is marked by a blue background. It is evident for any dimension d , the circuit complexity C_1 scales similarly. However higher the dimension d , larger is the value of C_1 at any particular time in the red region.

VI. Conclusions

The concluding remarks of this work are appended below point-wise:

- Focusing on a quenched quantum field theory, in this article we have derived the analytical expression for time-dependent quantum computational complexity using Nielsen's method viz., circuit complexity. Further, we have also discussed on various parametric variation of circuit complexity.
- Discretising the field theory on a lattice, we evaluated the time-dependent wavefunction for N -coupled oscillators having quartic perturbation and a quenched frequency. The wavefunction for the ground state of this system was derived using invariant operator method in a perturbative framework.
- The analytical form of the reference state and target states was chosen using the ground state wavefunction. Using a specific cost function and a minimal choice of basis, we could compute the exact form for the total complexity for two coupled oscillators. Further, we have computed the exact form of the unambiguous contribution of circuit complexity, for arbitrary, N number of oscillators.
- For two coupled oscillators, we observed that, in most part of the sudden quench, the total circuit complexity monotonously increases at very small values of quench rate, then scales linearly and shows a trend of thermalisation near $\delta t = 1$. In the slow quench limit, the complexity remains saturated irrespective of the quench rate. When parameterised for different values of quartic coupling, λ , it is evident that as coupling increases, even circuit complexity increases.
- The exact analytical form for unambiguous contribution of the circuit complexity for N coupled oscillators was derived using the results of [87]. The parametric variation of this circuit complexity was then plotted with respect to dimensionless parameter $(t/\delta t)$.

- It is evident from these plots that unambiguous contribution of the circuit complexity decreases with respect to the dimensionless parameter. When parametrised for different quartic couplings, we find that initially the complexity decreases linearly following same line, irrespective of the quartic coupling. Near to the quench point, complexity for each quartic coupling diverges and saturates at late times. After, quench point, the complexity after divergence is clearly in direct proportion to the increasing value of quartic coupling.
- We observed that, the unambiguous contribution of the circuit complexity behaves similarly, irrespective of the number of oscillators, N . However, as N increases the respective value of complexity increases at any particular time. Using this, we commented on the conitnum limit where the results would still be the same.
- Furthermore, it is clear that the unambiguous contribution of circuit complexity for the chosen set of parameters is proportional to the increasing number of dimension at early times. However at the quench point, unambiguous contribution of circuit complexity attains a constant value irrespective of the number of dimensions and thermalises at late times.

Future Prospects:

- In this work we explored the effects of quantum quench on QFT with quartic coupling, in the future it would be interesting to explore the effects of quantum quench on Krylov Complexity [134–138] for QFT with quartic coupling.
- Some of the works focusing on understanding the connection between complexity and quantum entanglement are [131, 139–142]. The connection between complexity and quantum entanglement in the case of quenched theories might turn out to be fruitful.

Acknowledgement: SC would like to thank the work friendly environment of CCSP, SGT University for providing tremendous support in research and offer the Assistant Professor (Senior Grade) position. SC also thanks all the members of our newly formed virtual international non-profit consortium Quantum Aspects of the Space-Time & Matter (QASTM) for elaborative discussions. RMG, SM and NP would like to thank the members of the QASTM Forum for useful discussions. Last but not least, we would like to acknowledge our debt to the people belonging to the various parts of the world for their generous and steady support for research in natural sciences.

A. $\mathcal{C}_{\kappa=1}^{(2)}$ in terms of renormalized parameters

As discussed in [87] one can attempt to find the form of $\mathcal{C}_{\kappa=1}^{(2)}$ by using renormalisation. In this subsection we give an outline of the modified expression for the same in case of a quenched interacting field theory discretised on a d -dimensional lattice containing N oscillators.

The renormalized matrix elements for A_2 block are given as [87],

$$A_2[m, n] = \frac{a_{mn} \lambda_R \delta^{-d}}{V^{\frac{1}{d-1}} f(\tilde{\omega}_i)}. \quad (\text{A1})$$

Note that all these elements are time-dependent due to the form of frequency, $\tilde{\omega}_i$ chosen as a quench profile. The eigenvalues then take the general form [87],

$$\Lambda_i^{(2)} = \frac{b_j \lambda_R \delta^{-d}}{V^{\frac{1}{d-1}} g(\tilde{\omega}_i)}, \quad (\text{A2})$$

where $j \in \{0, 1, \dots, (\text{Dim} A_2 - 1)\}$ while $i \in \{0, 1, \dots, N - 1\}$. As shown in [87] the renormalized penalty factor is,

$$\mathcal{A} = (\lambda_R \delta^{4-d})^\mu \delta^{-v} V^{\frac{v}{d-1}}. \quad (\text{A3})$$

Here v and μ are arbitrary integers which can be fixed by using physical arguments as discussed in [87]. Using Eq.(46), the renormalized-complexity contribution for A_2 block in d - dimensions can then be written as,

$$\mathcal{C}_{\kappa=1}^{(2)} = \frac{(\lambda_R \delta^{4-d})^\mu \delta^{-v} V^{\frac{v}{d-1}}}{2} \sum_{k=0}^{d-1} \sum_{i_k=0}^{(\text{Dim} A_2)-1} \left| \log \left(\frac{\Lambda_{i_k}^{(2)} \delta^2}{h_i \tilde{\omega}_{ref} \lambda_0} \right) \right|. \quad (\text{A4})$$

Note that now each $i_k \in \{1, 2, \dots, (\text{Dim} A_2 - 1)\}$ for $k \in \{1, 2, \dots, d - 1\}$. Using the renormalized form of eigenvalues from Eq.(A2) we finally obtain,

$$\mathcal{C}_{\kappa=1}^{(2)} = \frac{(\lambda_R \delta^{4-d})^\mu \delta^{-v} V^{\frac{v}{d-1}}}{2} \sum_{k=0}^{d-1} \sum_{i_k=0}^{(\text{Dim} A_2)-1} \left| \log \left(\frac{b_{i_k} \lambda_R \delta^{2-d}}{V^{\frac{1}{d-1}} g(\tilde{\omega}_i) h_{i_k} \tilde{\omega}_{ref} \lambda_0} \right) \right| \quad (\text{A5})$$

. Note that, we have not used this expression for getting numerically exact results.

B. Circuit Complexity for two oscillators

In the subsection IV A, we commented on the ambiguities in fixing the coefficients in the ambiguous A_2 block for arbitrary number of oscillators, N . Due to these ambiguities one cannot obtain numerical results for contribution from A_2 block in circuit complexity for N oscillators. However, in this appendix, we choose a minimal basis for the case of two oscillators and hence get rid of these ambiguities to get the total contribution of A_1 as well as A_2 block in circuit complexity. We begin by specialising the wavefunction (in normal modes) in Eq.(34) to that of two oscillators by inserting $N = 2$, written as:

$$\psi_{0,0}(\bar{x}_0, \bar{x}_1) = \frac{(g_0 g_1)^{1/4}}{\sqrt{\pi}} \exp[-\iota(\gamma_0 + \gamma_1)] \exp[C_0] \exp\left[-\frac{1}{2} \left(C_1 \bar{x}_0^2 + C_2 \bar{x}_1^2 + C_3 \bar{x}_0^2 \bar{x}_1^2 + C_4 \bar{x}_0^4 + C_5 \bar{x}_1^4 \right)\right]. \quad (\text{B1})$$

The exact form of C_i for $i = 0$ to $i = 5$ can be inferred from the table in the Appendix C. Next, we write the above wavefunction in the following form:

$$\psi^s(\bar{x}_0, \bar{x}_1) = \mathcal{N}^s \exp\left[-\frac{1}{2} \left(v_a A(s)_{ab} v_b \right)\right]. \quad (\text{B2})$$

Here \mathcal{N}^s is the normalisation factor. Similar to that of generalised wavefunction inserting $s = 1$ in the above equation will correspond to the target state, while inserting $s = 0$ corresponds to the reference state. We choose an unentangled and non-Gaussian reference state given by,

$$\psi^{s=0}(\bar{x}_0, \bar{x}_1) = \mathcal{N}^{s=0} \exp\left[-\frac{\tilde{\omega}_{ref}}{2} (\bar{x}_0^2 + \bar{x}_1^2 + \frac{\lambda_0}{2} (\bar{x}_0^4 + \bar{x}_1^4 + 6\bar{x}_0^2 \bar{x}_1^2))\right].$$

Here λ_0 parameterizes the non-Gaussianity of the reference state. The exponential in the above equation can be written in form of a matrix $A(s=0)$ by choosing a basis,

$$\vec{v} = \{\bar{x}_0, \bar{x}_1, \bar{x}_0\bar{x}_1, \bar{x}_0^2, \bar{x}_1^2\}. \quad (\text{B3})$$

The matrix then takes the following form:

$$A(s=0) = \begin{pmatrix} A_1^0 & 0 \\ 0 & A_2^0 \end{pmatrix}, \quad (\text{B4})$$

where,

$$A_1^0 = \begin{pmatrix} \tilde{\omega}_{ref} & 0 \\ 0 & \tilde{\omega}_{ref} \end{pmatrix} \quad ; \quad A_2^0 = \lambda_0 \tilde{\omega}_{ref} \begin{pmatrix} b & 0 & 0 \\ 0 & \frac{1}{2} & \frac{1}{2}(3-b) \\ 0 & \frac{1}{2}(3-b) & \frac{1}{2} \end{pmatrix}.$$

One can choose the values of b such that matrix A_2^0 is non-singular. To diagonalize A_2^0 we set $b = 3$. On the other hand to choose a non-Gaussian reference state we set $\lambda_0 = 1.5$.

Similarly one can get the target state in form of matrix $A(s=1)$ given by,

$$\psi^s(\bar{x}_0, \bar{x}_1) = \mathcal{N}^{s=1} \exp \left[-\frac{1}{2} \left(v_a A(s=1)_{ab} v_b \right) \right]. \quad (\text{B5})$$

Choosing the same basis as that in Eq.(B3) we can write the matrix for target state as,

$$A(s=1) = \begin{pmatrix} A_1^1 & 0 \\ 0 & A_2^1 \end{pmatrix}, \quad (\text{B6})$$

where,

$$A_1^1 = \begin{pmatrix} C_1 & 0 \\ 0 & C_2 \end{pmatrix} \quad ; \quad A_2^1 = \begin{pmatrix} \tilde{b}C_5 & 0 & 0 \\ 0 & C_3 & \frac{1}{2}(1-\tilde{b})C_5 \\ 0 & \frac{1}{2}(1-\tilde{b})C_5 & C_4 \end{pmatrix}.$$

The parameter \tilde{b} can be chosen such that A_2^1 is non-singular. Further to diagonalise A_2^1 we set $\tilde{b} = 1$. It is clear that with a minimal choice of basis given in Eq.(B3) one can fix all the elements of both A_1 and A_2 blocks for the case of two oscillators. Aimed with the expression for circuit complexity for N oscillators given in Eq.(46), and setting the penalty factor $\mathcal{A} = \infty$, we have computed the circuit complexity for the two quenched oscillators with quartic coupling, by using:

$$\mathcal{C}_{\kappa=1} = \frac{1}{2} \left(\log \left| \frac{\det A_1^1}{\det A_1^0} \right| + \log \left| \frac{\det A_2^1}{\det A_2^0} \right| \right). \quad (\text{B7})$$

Here *det* refers to the determinant of the respective block of the matrix. Note that the quench profile chosen as the frequency scale of the system imposes time-dependence on each element of the target state matrix block viz., A_1^1 and A_2^1 . The complexity therefore becomes time-dependent, this is clearly shown in the numerical results discussed in the section V.

C. Tabulated Values of Coefficients

In this appendix, the values of various coefficients we have used in some steps to compute the analytical expression of circuit complexity, are tabulated in respective tables.

- We begin by listing the values of B_i for $i = 1, 2, \dots, 5$ in equation Eq.(35) of section III B in the table given below.

B_i	Coefficient of B_i
$B_1(a)$	$-\frac{3x_a^2}{4Ng_aW_a} + \frac{9}{16Ng_a^2W_a} - \frac{x_a^4}{4NW_a}$
$B_2(b, c)$	$-\frac{3x_b^2W_c}{2NW_bg_c(W_b+W_c)} - \frac{3W_bx_c^2}{2Ng_bW_c(W_b+W_c)} + \frac{3}{4Ng_bg_c(W_b+W_c)} + \frac{3W_c}{4Ng_bW_bg_c(W_b+W_c)} + \frac{3W_b}{4Ng_bg_cW_c(W_b+W_c)} - \frac{3x_b^2x_c^2}{N(W_b+W_c)}$
$B_3(d, e)$	$-\frac{12x_dW_ex_e}{Ng_e(W_d+W_e)(W_d+3W_e)} - \frac{4x_dx_e^3}{N(W_d+3W_e)}$
$B_4(f, m, h)$	$-\frac{12x_fx_hW_m}{Ng_m(W_f+W_h)(W_f+W_h+2W_m)} - \frac{12x_fx_hx_m^2}{N(W_f+W_h+2W_m)}$
$B_5(i, j, k, l)$	$-\frac{24x_ix_jx_kx_l}{N(W_i+W_j+W_k+W_l)}$

Note that g_k for $k = 0, \dots, N-1$ is defined in the subsection III A, while W_k in Eq.(32). Also all the indices in the tabulated expressions run from 0 to $N-1$.

- Next, we tabulate the values of coefficients C_i for $i = 1, 2, \dots, 5$ in equation Eq.(B1) of the Appendix B.

C_i	Coefficient of C_i
C_0	$\frac{9\lambda}{32g_0^2W_0} + \frac{9\lambda}{32g_1^2W_1} + \frac{3\lambda}{8g_0g_1(W_0+W_1)} + \frac{3\lambda W_1}{8g_0g_1W_0(W_0+W_1)} + \frac{3\lambda W_0}{8g_0g_1W_1(W_0+W_1)}$
C_1	$-\frac{3\lambda}{8g_0W_0} - \frac{3\lambda W_1}{4g_1W_0(W_0+W_1)} - \frac{\nu_0}{2}$
C_2	$-\frac{3\lambda}{8g_1W_1} - \frac{3\lambda W_0}{4g_0W_1(W_0+W_1)} - \frac{\nu_1}{2}$
C_3	$-\frac{\lambda}{8W_0}$
C_4	$-\frac{\lambda}{8W_1}$
C_5	$-\frac{3\lambda}{2(W_0+W_1)}$

Note that $g_k = \hat{\gamma}_k$ where γ_k for $k = 0, 1$ can be computed by solving the EMP equation as shown in the section II, while W_k can be computed using Eq.(32).

[1] P. Calabrese and J. Cardy, "Entanglement entropy and quantum field theory," *Journal of Statistical*

- 2004) 06002, [arXiv:hep-th/0405152](#) [[hep-th](#)].
- [2] E. Witten, “Notes on Some Entanglement Properties of Quantum Field Theory,” *arXiv e-prints* (Mar., 2018) [arXiv:1803.04993](#), [arXiv:1803.04993](#) [[hep-th](#)].
- [3] T. Nishioka, “Entanglement entropy: Holography and renormalization group,” *Reviews of Modern Physics* **90** no. 3, (July, 2018) 035007, [arXiv:1801.10352](#) [[hep-th](#)].
- [4] D. Blanco, “Quantum information measures and their applications in quantum field theory,” *arXiv e-prints* (Feb., 2017) [arXiv:1702.07384](#), [arXiv:1702.07384](#) [[hep-th](#)].
- [5] M. Headrick, “Lectures on entanglement entropy in field theory and holography,” *arXiv e-prints* (July, 2019) [arXiv:1907.08126](#), [arXiv:1907.08126](#) [[hep-th](#)].
- [6] L. Amico, R. Fazio, A. Osterloh, and V. Vedral, “Entanglement in many-body systems,” *Reviews of Modern Physics* **80** no. 2, (Apr., 2008) 517–576, [arXiv:quant-ph/0703044](#) [[quant-ph](#)].
- [7] J. I. Cirac, “Entanglement in many-body quantum systems,” *arXiv e-prints* (May, 2012) [arXiv:1205.3742](#), [arXiv:1205.3742](#) [[quant-ph](#)].
- [8] A. Lakshminarayanan and V. Subrahmanyam, “Multipartite entanglement in a one-dimensional time-dependent ising model,” *Phys. Rev. A* **71** (Jun, 2005) 062334.
- [9] H. F. Song, S. Rachel, C. Flindt, I. Klich, N. Laflorencie, and K. Le Hur, “Bipartite fluctuations as a probe of many-body entanglement,” *Phys. Rev. B* **85** (Jan, 2012) 035409.
- [10] C. J. Bardeen, “Time dependent correlations of entangled states with nondegenerate branches and possible experimental realization using singlet fission,” *The Journal of Chemical Physics* **151** no. 12, (2019) 124503.
- [11] A. Sivaramakrishnan, “Entanglement entropy with a time-dependent hamiltonian,” *Phys. Rev. D* **97** (Mar, 2018) 066003.
- [12] P. Caputa, G. Mandal, and R. Sinha, “Dynamical entanglement entropy with angular momentum and U(1) charge,” *Journal of High Energy Physics* **2013** (Nov., 2013) 52, [arXiv:1306.4974](#) [[hep-th](#)].
- [13] E. Canovi, E. Ercolessi, P. Naldesi, L. Taddia, and D. Vodola, “Dynamics of entanglement entropy and entanglement spectrum crossing a quantum phase transition,” *Phys. Rev. B* **89** no. 10, (Mar., 2014) 104303, [arXiv:1311.3612](#) [[cond-mat.stat-mech](#)].
- [14] P. Jacquod and C. Petitjean, “Decoherence, entanglement and irreversibility in quantum dynamical systems with few degrees of freedom,” *Advances in Physics* **58** no. 2, (2009) 67–196.
- [15] S. Akhtar, S. Choudhury, S. Chowdhury, D. Goswami, S. Panda, and A. Swain, “Open Quantum Entanglement: A study of two atomic system in static patch of de Sitter space,” *Eur. Phys. J. C* **80** no. 8, (2020) 748, [arXiv:1908.09929](#) [[hep-th](#)].
- [16] S. Choudhury and S. Panda, “Quantum entanglement in de Sitter space from stringy axion: An analysis using α vacua,” *Nucl. Phys. B* **943** (2019) 114606, [arXiv:1712.08299](#) [[hep-th](#)].
- [17] S. Choudhury and S. Panda, “Entangled de Sitter from stringy axionic Bell pair I: an analysis using Bunch–Davies vacuum,” *Eur. Phys. J. C* **78** no. 1, (2018) 52, [arXiv:1708.02265](#) [[hep-th](#)].
- [18] S. Ghosh, K. S. Gupta, and S. C. L. Srivastava, “Entanglement dynamics following a sudden quench: An exact solution,” *EPL* **120** no. 5, (2017) 50005, [arXiv:1709.02202](#) [[quant-ph](#)].
- [19] S. Ghosh, K. S. Gupta, and S. C. L. Srivastava, “Exact relaxation dynamics and quantum information scrambling in multiply quenched harmonic chains,” *Phys. Rev. E* **100** no. 1, (2019) 012215, [arXiv:1905.06743](#) [[quant-ph](#)].
- [20] L. Susskind, “Three Lectures on Complexity and Black Holes,” 10, 2018. [arXiv:1810.11563](#) [[hep-th](#)].
- [21] A. R. Brown, L. Susskind, and Y. Zhao, “Quantum Complexity and Negative Curvature,” *Phys. Rev. D* **95** no. 4, (2017) 045010, [arXiv:1608.02612](#) [[hep-th](#)].
- [22] A. R. Brown, D. A. Roberts, L. Susskind, B. Swingle, and Y. Zhao, “Holographic Complexity Equals Bulk Action?,” *Phys. Rev. Lett.* **116** no. 19, (2016) 191301, [arXiv:1509.07876](#) [[hep-th](#)].
- [23] A. R. Brown, D. A. Roberts, L. Susskind, B. Swingle, and Y. Zhao, “Complexity, action, and black holes,” *Phys. Rev. D* **93** no. 8, (2016) 086006, [arXiv:1512.04993](#) [[hep-th](#)].
- [24] L. Susskind, “Entanglement is not enough,” *Fortsch. Phys.* **64** (2016) 49–71, [arXiv:1411.0690](#) [[hep-th](#)].
- [25] L. Susskind and Y. Zhao, “Switchbacks and the Bridge to Nowhere,” [arXiv:1408.2823](#) [[hep-th](#)].
- [26] D. Stanford and L. Susskind, “Complexity and Shock Wave Geometries,” *Phys. Rev. D* **90** no. 12, (2014) 126007, [arXiv:1406.2678](#) [[hep-th](#)].
- [27] L. Susskind, “Computational Complexity and Black Hole Horizons,” *Fortsch. Phys.* **64** (2016) 24–43, [arXiv:1403.5695](#) [[hep-th](#)]. [Addendum: *Fortsch.Phys.* 64, 44–48 (2016)].
- [28] J. L. F. Barbon and E. Rabinovici, “Holographic complexity and spacetime singularities,” *JHEP* **01** (2016) 084, [arXiv:1509.09291](#) [[hep-th](#)].
- [29] M. Alishahiha, “Holographic Complexity,” *Phys. Rev. D* **92** no. 12, (2015) 126009, [arXiv:1509.06614](#) [[hep-th](#)].
- [30] R.-Q. Yang, “Strong energy condition and complexity growth bound in holography,” *Phys. Rev. D* **95** no. 8, (2017) 086017, [arXiv:1610.05090](#) [[gr-qc](#)].
- [31] S. Chapman, H. Marrochio, and R. C. Myers, “Complexity of Formation in Holography,” *JHEP* **01** (2017) 062, [arXiv:1610.08063](#) [[hep-th](#)].
- [32] Y. Zhao, “Complexity and Boost Symmetry,” *Phys. Rev. D* **98** no. 8, (2018) 086011, [arXiv:1702.03957](#) [[hep-th](#)].
- [33] M. Flory, “A complexity/fidelity susceptibility g -theorem for AdS₃/BCFT₂,” *JHEP* **06** (2017) 131, [arXiv:1702.06386](#) [[hep-th](#)].
- [34] M. Alishahiha and A. Faraji Astaneh, “Holographic Fidelity Susceptibility,” *Phys. Rev. D* **96** no. 8, (2017) 086004, [arXiv:1705.01834](#) [[hep-th](#)].
- [35] A. Reynolds and S. F. Ross, “Complexity in de Sitter Space,” *Class. Quant. Grav.* **34** no. 17, (2017) 175013, [arXiv:1706.03788](#) [[hep-th](#)].
- [36] D. Carmi, S. Chapman, H. Marrochio, R. C. Myers, and S. Sugishita, “On the Time Dependence of Holographic Complexity,” *JHEP* **11** (2017) 188, [arXiv:1709.10184](#) [[hep-th](#)].
- [37] J. Couch, S. Eccles, W. Fischler, and M.-L. Xiao, “Holographic complexity and noncommutative gauge theory,” *JHEP* **03** (2018) 108, [arXiv:1710.07833](#)

- [hep-th].
- [38] R.-Q. Yang, C. Niu, C.-Y. Zhang, and K.-Y. Kim, “Comparison of holographic and field theoretic complexities for time dependent thermofield double states,” *JHEP* **02** (2018) 082, [arXiv:1710.00600 \[hep-th\]](#).
- [39] R. Abt, J. Erdmenger, H. Hinrichsen, C. M. Melby-Thompson, R. Meyer, C. Northe, and I. A. Reyes, “Topological Complexity in AdS₃/CFT₂,” *Fortsch. Phys.* **66** no. 6, (2018) 1800034, [arXiv:1710.01327 \[hep-th\]](#).
- [40] B. Swingle and Y. Wang, “Holographic Complexity of Einstein-Maxwell-Dilaton Gravity,” *JHEP* **09** (2018) 106, [arXiv:1712.09826 \[hep-th\]](#).
- [41] A. P. Reynolds and S. F. Ross, “Complexity of the AdS Soliton,” *Class. Quant. Grav.* **35** no. 9, (2018) 095006, [arXiv:1712.03732 \[hep-th\]](#).
- [42] Y.-S. An and R.-H. Peng, “Effect of the dilaton on holographic complexity growth,” *Phys. Rev. D* **97** no. 6, (2018) 066022, [arXiv:1801.03638 \[hep-th\]](#).
- [43] Z. Fu, A. Maloney, D. Marolf, H. Maxfield, and Z. Wang, “Holographic complexity is nonlocal,” *JHEP* **02** (2018) 072, [arXiv:1801.01137 \[hep-th\]](#).
- [44] B. Chen, W.-M. Li, R.-Q. Yang, C.-Y. Zhang, and S.-J. Zhang, “Holographic subregion complexity under a thermal quench,” *JHEP* **07** (2018) 034, [arXiv:1803.06680 \[hep-th\]](#).
- [45] B. Chen, W.-M. Li, R.-Q. Yang, C.-Y. Zhang, and S.-J. Zhang, “Holographic subregion complexity under a thermal quench,” *JHEP* **07** (2018) 034, [arXiv:1803.06680 \[hep-th\]](#).
- [46] K. Hashimoto, N. Iizuka, and S. Sugishita, “Thoughts on Holographic Complexity and its Basis-dependence,” *Phys. Rev. D* **98** no. 4, (2018) 046002, [arXiv:1805.04226 \[hep-th\]](#).
- [47] M. Flory and N. Miekley, “Complexity change under conformal transformations in AdS₃/CFT₂,” *JHEP* **05** (2019) 003, [arXiv:1806.08376 \[hep-th\]](#).
- [48] J. Couch, S. Eccles, T. Jacobson, and P. Nguyen, “Holographic Complexity and Volume,” *JHEP* **11** (2018) 044, [arXiv:1807.02186 \[hep-th\]](#).
- [49] S. A. Hosseini Mansoori, V. Jahnke, M. M. Qaemmaqami, and Y. D. Olivas, “Holographic Complexity of Anisotropic Black Branes,” *Phys. Rev. D* **100** no. 4, (2019) 046014, [arXiv:1808.00067 \[hep-th\]](#).
- [50] S. Chapman, H. Marrochio, and R. C. Myers, “Holographic complexity in Vaidya spacetimes. Part I,” *JHEP* **06** (2018) 046, [arXiv:1804.07410 \[hep-th\]](#).
- [51] S. Chapman, H. Marrochio, and R. C. Myers, “Holographic complexity in Vaidya spacetimes. Part II,” *JHEP* **06** (2018) 114, [arXiv:1805.07262 \[hep-th\]](#).
- [52] E. Caceres, S. Chapman, J. D. Couch, J. P. Hernandez, R. C. Myers, and S.-M. Ruan, “Complexity of Mixed States in QFT and Holography,” *JHEP* **03** (2020) 012, [arXiv:1909.10557 \[hep-th\]](#).
- [53] O. Ben-Ami and D. Carmi, “On Volumes of Subregions in Holography and Complexity,” *JHEP* **11** (2016) 129, [arXiv:1609.02514 \[hep-th\]](#).
- [54] F. J. G. Abad, M. Kulaxizi, and A. Parnachev, “On Complexity of Holographic Flavors,” *JHEP* **01** (2018) 127, [arXiv:1705.08424 \[hep-th\]](#).
- [55] R.-G. Cai, S.-M. Ruan, S.-J. Wang, R.-Q. Yang, and R.-H. Peng, “Action growth for AdS black holes,” *JHEP* **09** (2016) 161, [arXiv:1606.08307 \[gr-qc\]](#).
- [56] L. Lehner, R. C. Myers, E. Poisson, and R. D. Sorkin, “Gravitational action with null boundaries,” *Phys. Rev. D* **94** no. 8, (2016) 084046, [arXiv:1609.00207 \[hep-th\]](#).
- [57] M. Moosa, “Evolution of Complexity Following a Global Quench,” *JHEP* **03** (2018) 031, [arXiv:1711.02668 \[hep-th\]](#).
- [58] M. Moosa, “Divergences in the rate of complexification,” *Phys. Rev. D* **97** no. 10, (2018) 106016, [arXiv:1712.07137 \[hep-th\]](#).
- [59] K. Hashimoto, N. Iizuka, and S. Sugishita, “Time evolution of complexity in Abelian gauge theories,” *Phys. Rev. D* **96** no. 12, (2017) 126001, [arXiv:1707.03840 \[hep-th\]](#).
- [60] M. Guo, J. Hernandez, R. C. Myers, and S.-M. Ruan, “Circuit Complexity for Coherent States,” *JHEP* **10** (2018) 011, [arXiv:1807.07677 \[hep-th\]](#).
- [61] M. Doroudiani, A. Naseh, and R. Pirmoradian, “Complexity for Charged Thermofield Double States,” *JHEP* **01** (2020) 120, [arXiv:1910.08806 \[hep-th\]](#).
- [62] T. Ali, A. Bhattacharyya, S. S. Haque, E. H. Kim, N. Moynihan, and J. Murugan, “Chaos and Complexity in Quantum Mechanics,” *Phys. Rev. D* **101** no. 2, (2020) 026021, [arXiv:1905.13534 \[hep-th\]](#).
- [63] S. Choudhury, A. Dutta, and D. Ray, “Chaos and Complexity from Quantum Neural Network: A study with Diffusion Metric in Machine Learning,” *JHEP* **04** (2021) 138, [arXiv:2011.07145 \[hep-th\]](#).
- [64] S. Chapman and H. Z. Chen, “Charged Complexity and the Thermofield Double State,” *JHEP* **02** (2021) 187, [arXiv:1910.07508 \[hep-th\]](#).
- [65] P. Bhargava, S. Choudhury, S. Chowdhury, A. Mishara, S. P. Selvam, S. Panda, and G. D. Pasquino, “Quantum aspects of chaos and complexity from bouncing cosmology: A study with two-mode single field squeezed state formalism,” [arXiv:2009.03893 \[hep-th\]](#).
- [66] J.-L. Lehnert and J. Quintin, “Quantum Circuit Complexity of Primordial Perturbations,” *Phys. Rev. D* **103** no. 6, (2021) 063527, [arXiv:2012.04911 \[hep-th\]](#).
- [67] A. Bhattacharyya, S. Das, S. S. Haque, and B. Underwood, “Rise of cosmological complexity: Saturation of growth and chaos,” *Phys. Rev. Res.* **2** no. 3, (2020) 033273, [arXiv:2005.10854 \[hep-th\]](#).
- [68] S. Choudhury, S. Chowdhury, N. Gupta, A. Mishara, S. P. Selvam, S. Panda, G. D. Pasquino, C. Singha, and A. Swain, “Circuit Complexity From Cosmological Islands,” *Symmetry* **13** (2021) 1301, [arXiv:2012.10234 \[hep-th\]](#).
- [69] K. Adhikari, S. Choudhury, S. Chowdhury, K. Shirish, and A. Swain, “Circuit complexity as a novel probe of quantum entanglement: A study with black hole gas in arbitrary dimensions,” *Phys. Rev. D* **104** no. 6, (2021) 065002, [arXiv:2104.13940 \[hep-th\]](#).
- [70] K. Adhikari, S. Choudhury, S. Chowdhury, K. Shirish, and A. Swain, “Circuit complexity as a novel probe of quantum entanglement: A study with black hole gas in arbitrary dimensions,” *Phys. Rev. D* **104** no. 6, (2021) 065002, [arXiv:2104.13940 \[hep-th\]](#).
- [71] K. Adhikari, S. Choudhury, H. N. Pandya, and

- R. Srivastava, “PGW Circuit Complexity,” [arXiv:2108.10334 \[gr-qc\]](#).
- [72] K. Y. Bhagat, B. Bose, S. Choudhury, S. Chowdhury, R. N. Das, S. G. Dastider, N. Gupta, A. Maji, G. D. Pasquino, and S. Paul, “The Generalized OTOC from Supersymmetric Quantum Mechanics—Study of Random Fluctuations from Eigenstate Representation of Correlation Functions,” *Symmetry* **13** no. 1, (2020) 44, [arXiv:2008.03280 \[hep-th\]](#).
- [73] J. Boruch, P. Caputa, D. Ge, and T. Takayanagi, “Holographic path-integral optimization,” *JHEP* **07** (2021) 016, [arXiv:2104.00010 \[hep-th\]](#).
- [74] J. Boruch, P. Caputa, and T. Takayanagi, “Path-Integral Optimization from Hartle-Hawking Wave Function,” *Phys. Rev. D* **103** no. 4, (2021) 046017, [arXiv:2011.08188 \[hep-th\]](#).
- [75] S. Choudhury, S. P. Selvam, and K. Shirish, “Circuit Complexity From Supersymmetric Quantum Field Theory With Morse Function,” [arXiv:2101.12582 \[hep-th\]](#).
- [76] P. Caputa, N. Kundu, M. Miyaji, T. Takayanagi, and K. Watanabe, “Liouville Action as Path-Integral Complexity: From Continuous Tensor Networks to AdS/CFT,” *JHEP* **11** (2017) 097, [arXiv:1706.07056 \[hep-th\]](#).
- [77] P. Caputa and J. M. Magan, “Quantum Computation as Gravity,” *Phys. Rev. Lett.* **122** no. 23, (2019) 231302, [arXiv:1807.04422 \[hep-th\]](#).
- [78] P. Caputa and I. MacCormack, “Geometry and Complexity of Path Integrals in Inhomogeneous CFTs,” *JHEP* **01** (2021) 027, [arXiv:2004.04698 \[hep-th\]](#).
- [79] R. Khan, C. Krishnan, and S. Sharma, “Circuit Complexity in Fermionic Field Theory,” *Phys. Rev. D* **98** no. 12, (2018) 126001, [arXiv:1801.07620 \[hep-th\]](#).
- [80] K. Adhikari, S. Choudhury, S. Kumar, S. Mandal, N. Pandey, A. Roy, S. Sarkar, P. Sarker, and S. S. Shariff, “Circuit Complexity in $\mathcal{Z}_2\mathcal{EFT}$,” [arXiv:2109.09759 \[hep-th\]](#).
- [81] K. Adhikari, S. Choudhury, and A. Roy, “ \mathcal{K} Crylov Complexity in Quantum Field Theory,” [arXiv:2204.02250 \[hep-th\]](#).
- [82] K. Adhikari, S. Choudhury, H. N. Pandya, and R. Srivastava, “PGW Circuit Complexity,” [arXiv:2108.10334 \[gr-qc\]](#).
- [83] S. Choudhury, A. Mukherjee, N. Pandey, and A. Roy, “Causality Constraint on Circuit Complexity from $\mathcal{COSMOEFT}$,” [arXiv:2111.11468 \[hep-th\]](#).
- [84] R. Jefferson and R. C. Myers, “Circuit complexity in quantum field theory,” *JHEP* **10** (2017) 107, [arXiv:1707.08570 \[hep-th\]](#).
- [85] L. Hackl and R. C. Myers, “Circuit complexity for free fermions,” *JHEP* **07** (2018) 139, [arXiv:1803.10638 \[hep-th\]](#).
- [86] S. Chapman, M. P. Heller, H. Marrochio, and F. Pastawski, “Toward a Definition of Complexity for Quantum Field Theory States,” *Phys. Rev. Lett.* **120** no. 12, (2018) 121602, [arXiv:1707.08582 \[hep-th\]](#).
- [87] A. Bhattacharyya, A. Shekar, and A. Sinha, “Circuit complexity in interacting QFTs and RG flows,” *JHEP* **10** (2018) 140, [arXiv:1808.03105 \[hep-th\]](#).
- [88] A. Polkovnikov, K. Sengupta, A. Silva, and M. Vengalattore, “Colloquium: Nonequilibrium dynamics of closed interacting quantum systems,” *Rev. Mod. Phys.* **83** (Aug, 2011) 863–883.
- [89] C. Gogolin and J. Eisert, “Equilibration, thermalisation, and the emergence of statistical mechanics in closed quantum systems,” *Reports on Progress in Physics* **79** no. 5, (Apr, 2016) 056001.
- [90] P. Calabrese, F. H. L. Essler, and G. Mussardo, “Introduction to ‘quantum integrability in out of equilibrium systems’,” *Journal of Statistical Mechanics: Theory and Experiment* **2016** no. 6, (Jun, 2016) 064001.
- [91] P. Calabrese and J. Cardy, “Quantum Quenches in Extended Systems,” *J. Stat. Mech.* **0706** (2007) P06008, [arXiv:0704.1880 \[cond-mat.stat-mech\]](#).
- [92] P. Basu and S. R. Das, “Quantum Quench across a Holographic Critical Point,” *JHEP* **01** (2012) 103, [arXiv:1109.3909 \[hep-th\]](#).
- [93] A. Buchel, L. Lehner, R. C. Myers, and A. van Niekerk, “Quantum quenches of holographic plasmas,” *JHEP* **05** (2013) 067, [arXiv:1302.2924 \[hep-th\]](#).
- [94] S. R. Das, D. A. Galante, and R. C. Myers, “Universal scaling in fast quantum quenches in conformal field theories,” *Phys. Rev. Lett.* **112** (2014) 171601, [arXiv:1401.0560 \[hep-th\]](#).
- [95] S. R. Das, D. A. Galante, and R. C. Myers, “Universality in fast quantum quenches,” *JHEP* **02** (2015) 167, [arXiv:1411.7710 \[hep-th\]](#).
- [96] S. R. Das, D. A. Galante, and R. C. Myers, “Smooth and fast versus instantaneous quenches in quantum field theory,” *JHEP* **08** (2015) 073, [arXiv:1505.05224 \[hep-th\]](#).
- [97] S. R. Das, D. A. Galante, and R. C. Myers, “Quantum Quenches in Free Field Theory: Universal Scaling at Any Rate,” *JHEP* **05** (2016) 164, [arXiv:1602.08547 \[hep-th\]](#).
- [98] V. Alba and P. Calabrese, “Entanglement dynamics after quantum quenches in generic integrable systems,” *SciPost Physics* **4** no. 3, (Mar., 2018) 017, [arXiv:1712.07529 \[cond-mat.stat-mech\]](#).
- [99] S. Choudhury, R. M. Gharat, S. Mandal, N. Pandey, A. Roy, and P. Sarker, “Entanglement in interacting quenched two-body coupled oscillator system,” *Phys. Rev. D* **106** no. 2, (July, 2022) 025002, [arXiv:2204.05326 \[hep-th\]](#).
- [100] H. A. Camargo, P. Caputa, D. Das, M. P. Heller, and R. Jefferson, “Complexity as a Novel Probe of Quantum Quenches: Universal Scalings and Purifications,” *Phys. Rev. Lett.* **122** no. 8, (Mar., 2019) 081601, [arXiv:1807.07075 \[hep-th\]](#).
- [101] D. W. F. Alves and G. Camilo, “Evolution of complexity following a quantum quench in free field theory,” *Journal of High Energy Physics* **2018** no. 6, (June, 2018) 29, [arXiv:1804.00107 \[hep-th\]](#).
- [102] T. Langen, T. Gasenzer, and J. Schmiedmayer, “Prethermalization and universal dynamics in near-integrable quantum systems,” *Journal of Statistical Mechanics: Theory and Experiment* **2016** no. 6, (Jun, 2016) 064009.
- [103] T. Kinoshita, T. Wenger, and D. Weiss, “A quantum newton’s cradle,” *Nature* **440** (05, 2006) 900–3.
- [104] S. Hofferberth, I. Lesanovsky, B. Fischer, T. Schumm, and J. Schmiedmayer, “Non-equilibrium coherence dynamics in one-dimensional Bose gases,” *Nature (London)* **449** no. 7160, (Sept., 2007) 324–327,

- [arXiv:0706.2259 \[cond-mat.other\]](#).
- [105] S. Trotzky, Y. A. Chen, A. Flesch, I. P. McCulloch, U. Schollwöck, J. Eisert, and I. Bloch, “Probing the relaxation towards equilibrium in an isolated strongly correlated one-dimensional Bose gas,” *Nature Physics* **8** no. 4, (Apr., 2012) 325–330, [arXiv:1101.2659 \[cond-mat.quant-gas\]](#).
- [106] M. Gring, M. Kuhnert, T. Langen, T. Kitagawa, B. Rauer, M. Schreitl, I. Mazets, D. A. Smith, E. Demler, and J. Schmiedmayer, “Relaxation and prethermalization in an isolated quantum system,” *Science* **337** no. 6100, (2012) 1318–1322.
- [107] M. Cheneau, P. Barmettler, D. Poletti, M. Endres, P. Schauß, T. Fukuhara, C. Gross, I. Bloch, C. Kollath, and S. Kuhr, “Light-cone-like spreading of correlations in a quantum many-body system,” *Nature (London)* **481** no. 7382, (Jan., 2012) 484–487, [arXiv:1111.0776 \[cond-mat.quant-gas\]](#).
- [108] F. Meinert, M. J. Mark, E. Kirilov, K. Lauber, P. Weinmann, A. J. Daley, and H.-C. Nägerl, “Quantum quench in an atomic one-dimensional ising chain,” *Phys. Rev. Lett.* **111** (Jul, 2013) 053003.
- [109] T. Langen, R. Geiger, M. Kuhnert, B. Rauer, and J. Schmiedmayer, “Local emergence of thermal correlations in an isolated quantum many-body system,” *Nature Physics* **9** no. 10, (Oct., 2013) 640–643, [arXiv:1305.3708 \[cond-mat.quant-gas\]](#).
- [110] T. Fukuhara, P. Schauß, M. Endres, S. Hild, M. Cheneau, I. Bloch, and C. Gross, “Microscopic observation of magnon bound states and their dynamics,” *Nature (London)* **502** no. 7469, (Oct., 2013) 76–79, [arXiv:1305.6598 \[cond-mat.quant-gas\]](#).
- [111] T. Fukuhara, A. Kantian, M. Endres, M. Cheneau, P. Schauß, S. Hild, D. Bellem, U. Schollwöck, T. Giamarchi, C. Gross, I. Bloch, and S. Kuhr, “Quantum dynamics of a mobile spin impurity,” *Nature Physics* **9** no. 4, (Apr., 2013) 235–241, [arXiv:1209.6468 \[cond-mat.quant-gas\]](#).
- [112] H. R. Lewis and W. B. Riesenfeld, “An exact quantum theory of the time-dependent harmonic oscillator and of a charged particle in a time-dependent electromagnetic field,” *Journal of Mathematical Physics* **10** no. 8, (1969) 1458–1473.
- [113] K. Andrzejewski, “Dynamics of entropy and information of time-dependent quantum systems: exact results,” *Quant. Inf. Proc.* **21** no. 3, (2022) 117, [arXiv:2108.00975 \[quant-ph\]](#).
- [114] B. Khantoul, A. Bounames, and M. Maamache, “On the invariant method for the time-dependent non-Hermitian Hamiltonians,” *European Physical Journal Plus* **132** no. 6, (June, 2017) 258, [arXiv:1610.09273 \[quant-ph\]](#).
- [115] S. Choudhury, “Cosmological Geometric Phase From Pure Quantum States: A study without/with having Bell’s inequality violation,” [arXiv:2105.06254 \[gr-qc\]](#).
- [116] J.-R. Choi, “Coherent and squeezed states for light in homogeneous conducting linear media by an invariant operator method,” *International Journal of Theoretical Physics* **43** no. 10, (2004) 2113–2136.
- [117] H. Kanasugi and H. Okada, “Systematic Treatment of General Time-Dependent Harmonic Oscillator in Classical and Quantum Mechanics,” *Progress of Theoretical Physics* **93** no. 5, (05, 1995) 949–960.
- [118] “Adiabatic evolution under quantum control,” *Annals of Physics* **327** no. 5, (2012) 1293–1303.
- [119] M.-Y. Ye, X.-F. Zhou, Y.-S. Zhang, and G.-C. Guo, “Two kinds of quantum adiabatic approximation,” *Physics Letters A* **368** no. 1, (2007) 18–24.
- [120] J. R. Choi, “Perturbation theory for time-dependent quantum systems involving complex potentials,” *Frontiers in Physics* **8** (June, 2020) 189.
- [121] V. P. Ermakov, “Second-order differential equations: conditions of complete integrability,” *Applicable Analysis and Discrete Mathematics* (2008) 123–145.
- [122] W. Milne, “The numerical determination of characteristic numbers,” *Physical Review* **35** no. 7, (1930) 863.
- [123] E. Pinney, “The nonlinear differential equation $y'' + p(x)y' + cy - 3 = 0$,” in *Proc. Amer. Math. Soc.*, vol. 1, pp. 681–681. 1950.
- [124] M. A. Nielsen, “A geometric approach to quantum circuit lower bounds,” [quant-ph/0502070](#).
- [125] M. A. Nielsen, “Quantum computation as geometry,” *Science* **311** no. 5764, (Feb, 2006) 1133–1135, [quant-ph/0603161](#).
- [126] M. R. Dowling and M. A. Nielsen, “The geometry of quantum computation,” *Quantum Info. Comput.* **8** no. 10, (Nov., 2008) 861–899, [quant-ph/070100](#).
- [127] M. A. Nielsen, M. R. Dowling, M. Gu, and A. C. Doherty, “Optimal control, geometry, and quantum computing,” *Phys. Rev. A* **73** (Jun, 2006) 062323, [quant-ph/0603160](#).
- [128] M. A. Nielsen, “A Geometric Approach to Quantum Circuit Lower Bounds,” [arXiv:quant-ph/0502070 \[quant-ph\]](#).
- [129] R. A. Jefferson and R. C. Myers, “Circuit complexity in quantum field theory,” *Journal of High Energy Physics* **2017** no. 10, (Oct., 2017) 107, [arXiv:1707.08570 \[hep-th\]](#).
- [130] P. Caputa, S. R. Das, M. Nozaki, and A. Tomiya, “Quantum Quench and Scaling of Entanglement Entropy,” *Phys. Lett. B* **772** (2017) 53–57, [arXiv:1702.04359 \[hep-th\]](#).
- [131] H. A. Camargo, P. Caputa, D. Das, M. P. Heller, and R. Jefferson, “Complexity as a novel probe of quantum quenches: Universal scalings and purifications,” *Phys. Rev. Lett.* **122** (Feb, 2019) 081601.
- [132] K. H. Yeon, H. J. Kim, C. I. Um, T. F. George, and L. N. Pandey, “Wave function in the invariant representation and squeezed-state function of the time-dependent harmonic oscillator,” *Phys. Rev. A* **50** no. 2, (Aug., 1994) 1035–1039.
- [133] S. Mukherjee, A. Ghose Choudhury, and P. Guha, “Generalized damped Milne-Pinney equation and Chiellini method,” *arXiv e-prints* (Mar., 2016) [arXiv:1603.08747](#), [arXiv:1603.08747 \[nlin.SI\]](#).
- [134] D. E. Parker, X. Cao, A. Avdoshkin, T. Scaffidi, and E. Altman, “A Universal Operator Growth Hypothesis,” *Phys. Rev. X* **9** no. 4, (2019) 041017, [arXiv:1812.08657 \[cond-mat.stat-mech\]](#).
- [135] P. Caputa and S. Liu, “Quantum complexity and topological phases of matter,” [arXiv:2205.05688 \[hep-th\]](#).
- [136] P. Caputa, J. M. Magan, and D. Patramanis, “Geometry of Krylov complexity,” *Phys. Rev. Res.* **4** no. 1, (2022) 013041, [arXiv:2109.03824 \[hep-th\]](#).

- [137] K. Adhikari, S. Choudhury, and A. Roy, “Krylov Complexity in Quantum Field Theory,” [arXiv:2204.02250 \[hep-th\]](#).
- [138] K. Adhikari and S. Choudhury, “Cosmological Krylov Complexity,” [arXiv:2203.14330 \[hep-th\]](#).
- [139] K. Adhikari, S. Choudhury, S. Chowdhury, K. Shirish, and A. Swain, “Circuit complexity as a novel probe of quantum entanglement: A study with black hole gas in arbitrary dimensions,” *Phys. Rev. D* **104** no. 6, (2021) 065002, [arXiv:2104.13940 \[hep-th\]](#).
- [140] S. Choudhury, S. Chowdhury, N. Gupta, A. Mishara, S. P. Selvam, S. Panda, G. D. Pasquino, C. Singha, and A. Swain, “Circuit Complexity from Cosmological Islands,” *Symmetry* **13** no. 7, (2021) 1301, [arXiv:2012.10234 \[hep-th\]](#).
- [141] J. Eisert, “Entangling Power and Quantum Circuit Complexity,” *Phys. Rev. Lett.* **127** no. 2, (July, 2021) 020501, [arXiv:2104.03332 \[quant-ph\]](#).
- [142] S. D. Mathur, “Three puzzles in cosmology,” *International Journal of Modern Physics D* **29** no. 14, (Jan., 2020) 2030013, [arXiv:2009.09832 \[hep-th\]](#).